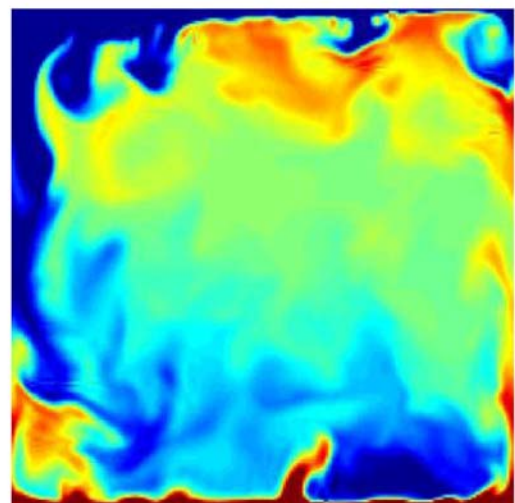
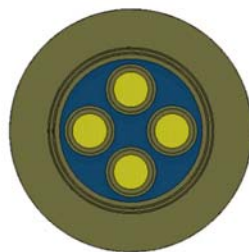
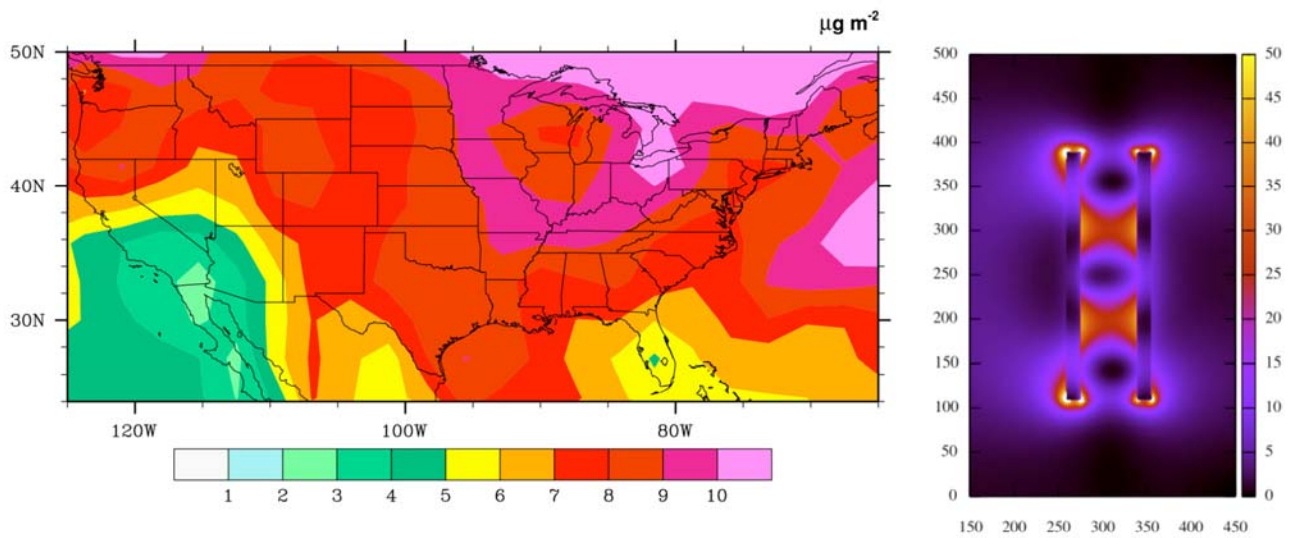


Argonne's Laboratory Computing Resource Center

2009 Annual Report



About Argonne National Laboratory

Argonne is a U.S. Department of Energy laboratory managed by UChicago Argonne, LLC under contract DE-AC02-06CH11357. The Laboratory's main facility is outside Chicago, at 9700 South Cass Avenue, Argonne, Illinois 60439. For information about Argonne, see www.anl.gov.

Availability of This Report

This report is available, at no cost, at <http://www.osti.gov/bridge>. It is also available on paper to the U.S. Department of Energy and its contractors, for a processing fee, from:

U.S. Department of Energy

Office of Scientific and Technical Information

P.O. Box 62

Oak Ridge, TN 37831-0062

phone (865) 576-8401

fax (865) 576-5728

reports@adonis.osti.gov

Disclaimer

This report was prepared as an account of work sponsored by an agency of the United States Government. Neither the United States Government nor any agency thereof, nor UChicago Argonne, LLC, nor any of their employees or officers, makes any warranty, express or implied, or assumes any legal liability or responsibility for the accuracy, completeness, or usefulness of any information, apparatus, product, or process disclosed, or represents that its use would not infringe privately owned rights. Reference herein to any specific commercial product, process, or service by trade name, trademark, manufacturer, or otherwise, does not necessarily constitute or imply its endorsement, recommendation, or favoring by the United States Government or any agency thereof. The views and opinions of document authors expressed herein do not necessarily state or reflect those of the United States Government or any agency thereof, Argonne National Laboratory, or UChicago Argonne, LLC.

Argonne's Laboratory Computing Resource Center

FY2009 Report

Now in its seventh year of operation, the Laboratory Computing Resource Center (LCRC) continues to be an integral component of science and engineering research at Argonne, supporting a diverse portfolio of projects for the U.S. Department of Energy and other sponsors. The LCRC's ongoing mission is to enable and promote computational science and engineering across the Laboratory, primarily by operating computing facilities and supporting high-performance computing application use and development. This report describes scientific activities carried out with LCRC resources in 2009 and the broad impact on programs across the Laboratory.

The LCRC computing facility, Jazz, is available to the entire Laboratory community. In addition, the LCRC staff provides training in high-performance computing and guidance on application usage, code porting, and algorithm development. All Argonne personnel and collaborators are encouraged to take advantage of this computing resource and to provide input into the vision and plans for computing and computational analysis at Argonne.

The LCRC Allocations Committee makes decisions on individual project allocations for Jazz. Committee members are appointed by the Associate Laboratory Directors and span a range of computational disciplines.

The 350-node LCRC cluster, Jazz, began production service in April 2003 and has been a research work horse ever since. Hosting a wealth of software tools and applications and achieving high availability year after year, researchers can count on Jazz to achieve project milestones and enable breakthroughs. Over the years, many projects have achieved results that would have been unobtainable without such a computing resource. In fiscal year 2009, there were 49 active projects representing a wide cross-section of Laboratory research and almost all research divisions.

For further information about the LCRC and Jazz, please see the LCRC Web site at <http://www.lcrc.anl.gov/>, or send e-mail to support@lrcr.anl.gov.

Ray Bair
Director, Laboratory Computing Resource Center
bair@lrcr.anl.gov

Table of Contents

2009 Scientific and Engineering Applications with LCRC

Atmospheric Chemistry and Transport	1
Spatiotemporal Chaos and Turbulence in Fluids.....	3
Simulations of High Energy Collider Physics Processes	6
Density Functional Theory Calculations of Electrocatalytic and Nanocatalytic Phenomena	7
DFT Screening Investigation of Catalytic and Electrocatalytic Phenomena of Transition Metals..	9
Global Climate Modeling with the Fast Ocean Atmosphere Model	10
HEIGHTS-3D Modeling	12
Mechanisms of CO Hydrogenation by Homogeneous Cobalt Catalysts.....	13
Hydrogenation	13
Studies of Voltage-Gated Potassium Channels	15
Lattice Quantum Chromodynamics.....	16
Lithium-Ion Battery Electrode Modeling.....	17
Monte Carlo Characterization of Accelerator-Driven Subcritical Facilities	19
Energy Production from Spent Nuclear Fuels and Transmutation of Long-Lived Fission Products	21
Coarse-Graining Methods for Molecular Dynamics and Their Application to Ion-Channel Proteins	24
Computational Nanophotonics	25
Neocortical Seizure Simulation.....	26
Optimization of Many-Body Wavefunctions	28
Parallel Tools Performance Testing	29
Parallel Implicit Algorithms in Edge Fusion Simulations	30
Quantum Monte Carlo Calculations of Light Nuclei	31
Safety Analysis Report Review of Radioactive Material Packaging	33
Toolkit for Advanced Optimization	34
Uncertainty in Weather Forecasting.....	35
Optimization of Nuclear-Energy DFT Functionals.....	36
Multimethod Linear Solvers in Large-Scale PDE-Based Simulations.....	38

Atmospheric Chemistry and Transport

PIs: Veerabhadra Kotamarthi and Beth Drewniak (Environmental Science)

We are using three-dimensional models of the atmospheric dynamics, chemistry, and transport to evaluate the impacts of energy-related and biogenic emissions on the urban and regional- and global-scale environments. During 2009 we used MOZART, a global-scale chemistry transport code, to model estimates of mercury flux into the United States from nonlocal and global sources. The results are shown in Figure 1. Our studies indicated that a sixth of the mercury now falling on North American lakes comes from Asia, particularly China, mainly from coal-fired plants and smelters but also from incinerators. The work received national coverage in the *New York Times* (<http://www.nytimes.com/2009/08/12/business/energy-environment/12incinerate.html>).

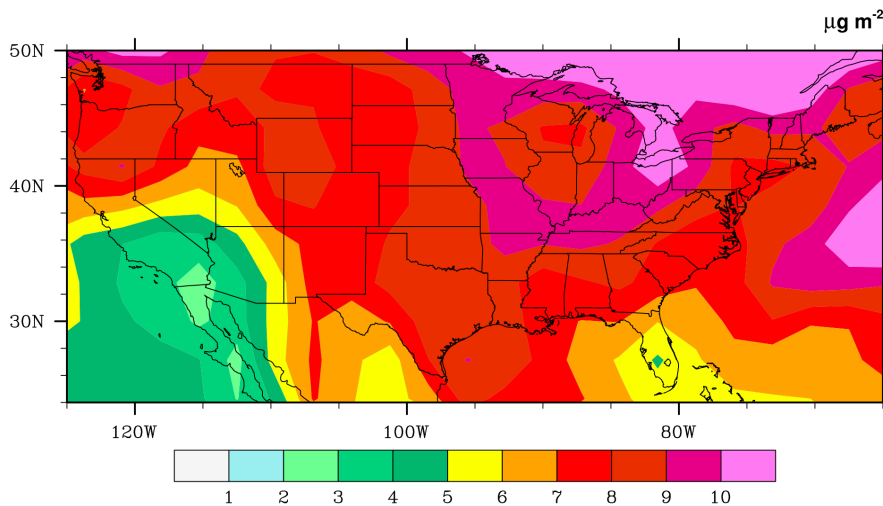


Figure 1: Wet deposition pattern follows the measurements from the MDN network and within the range measured. (Some high, measured wet deposition rates over Florida are not reported.) These results are similar to the calculated results of Seignuer *et al.* (2001) using a global model and without any scaling for the precipitation in the model with observations.

In another study, we used the Jazz resources to simulate the PM₁₀ pollution (pollution from particulate matter with an aerodynamic diameter smaller than or equal to 10 micrometers) in South Korea. The emissions for this study were prepared by using the Environmental Protection Agency emission modeling software SMOKE and additional data from Dr. Deng. The calculated emissions and a year-long run of MM5 mesoscale model were used as inputs to a regional chemical transport model, named CMAQ. The model simulations (Figs. 2–3) show reasonable agreement for ozone and PM₁₀ particulate pollution at several stations in Seoul, South Korea.

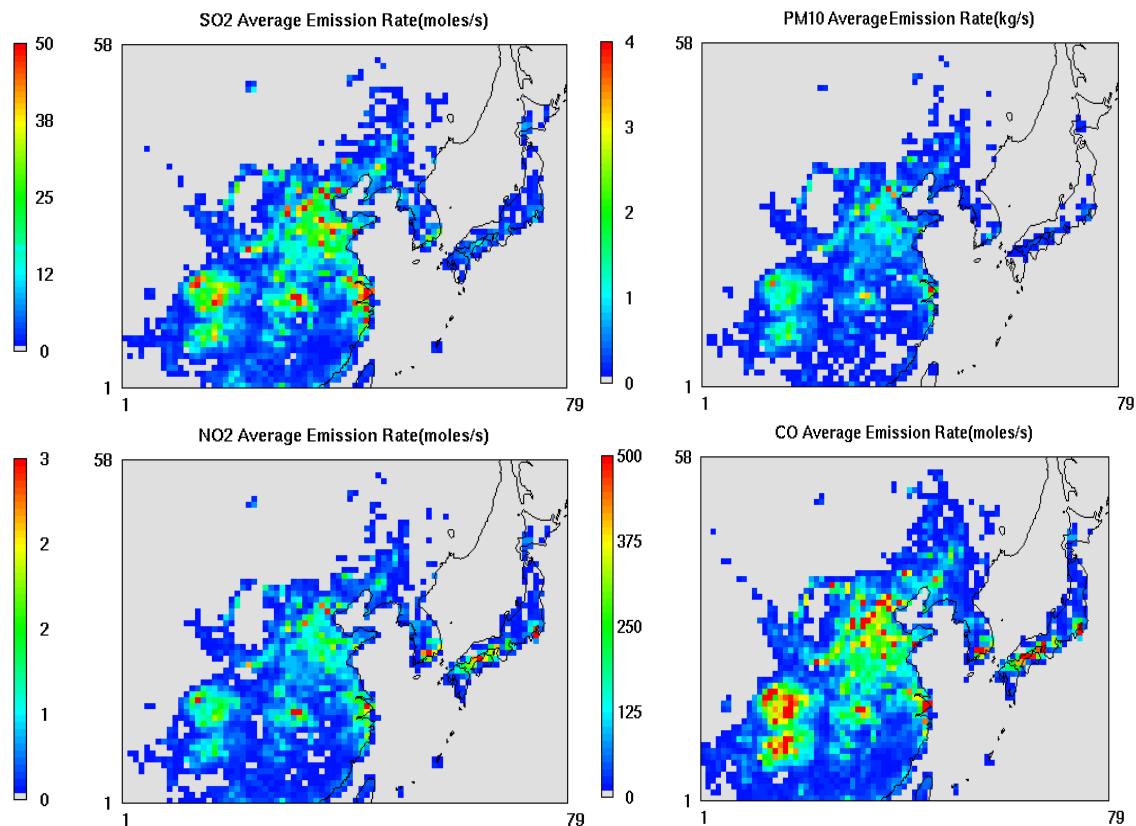


Figure 2: Calculated emissions of SO_2 , PM_{10} , NO_x , and CO for the three domains in the model.

Publications and Presentations

M. Franklin, D. Cook and V. R. Kotamarthi, Characterizing flux measurements for validating climate model parameterizations, Poster presentation, *Climate Change and Prediction Program Meeting*, Bethesda, Maryland, April 6–9, 2009.

Dong Young Kim, Youngsoo Chang, Veerabhadra R. Kotamarthi, Simulation of background PM_{10} in Seoul metropolitan area, Korea using modeling system MM5-CMAQ, Preprint, 2009.

R. Kotamarthi, M. Franklin, D. Cook, and M. L. Stein, High-spatial-resolution data sets for climate model evaluation: Data ensembles for sparse measurements, Poster presentation, *Climate Change and Prediction Program Meeting*, Bethesda, Maryland, April 6–9, 2009.

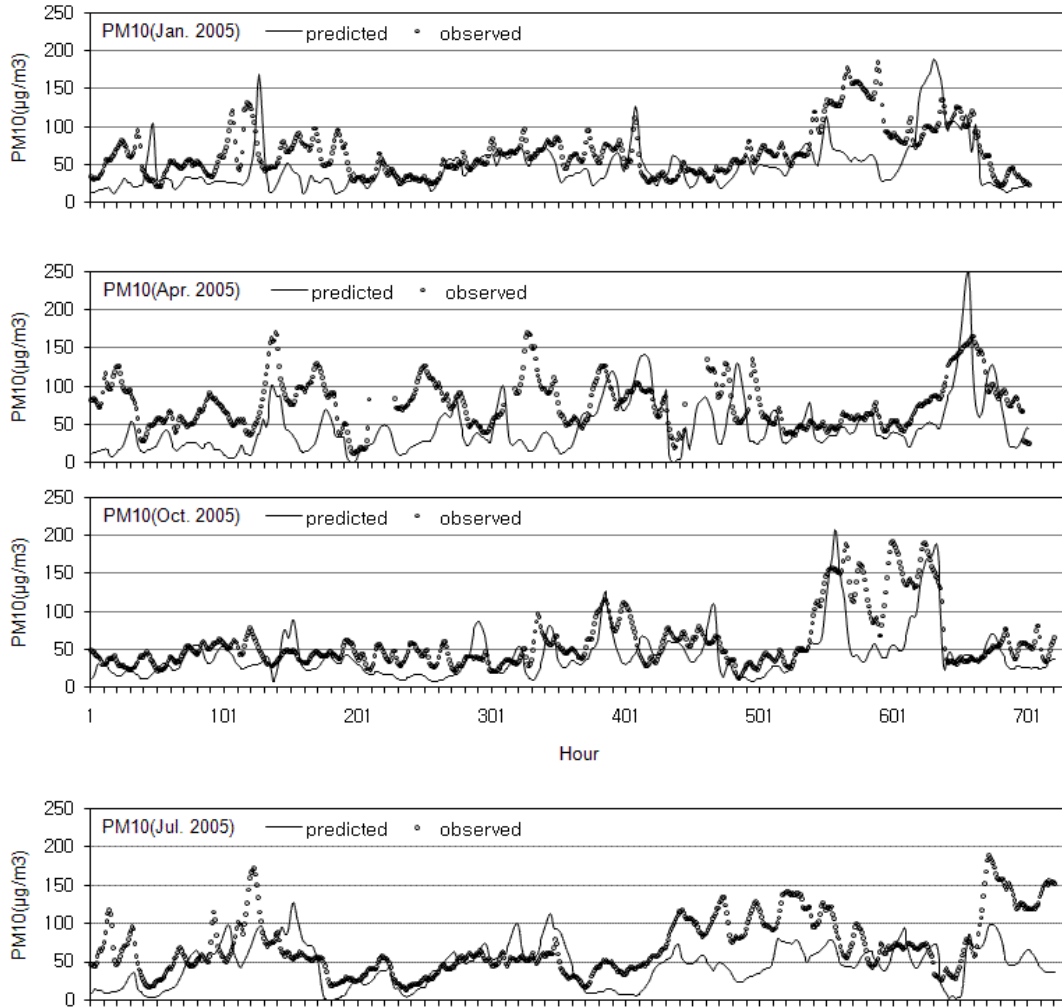


Figure 3: Measured and observed PM10 at locations near Seoul for different months of the year.

Spatiotemporal Chaos and Turbulence in Fluids

PIs: Mark Paul (Virginia Tech) and Paul Fischer (Mathematics and Computer Science)

We are studying open questions in spatiotemporal chaos and turbulence using large-scale numerical simulations of Rayleigh-Benard convection (a thin horizontal layer of fluid warmed uniformly from below and cooled uniformly from above). Turbulent Rayleigh-Benard systems occur in such diverse phenomena as heat exchangers in power plants, melting processes, and natural convection in the atmosphere. We are performing numerical simulations for experimentally realistic conditions using a highly optimized spectral element code. An overarching theme of our work is to provide a quantitative link between theory and experiment. Many theoretical predictions are for idealized situations that are approximations to the conditions

of experiment. By performing simulations for the same conditions of experiment, we can test quantitatively with theoretical predictions. In addition, our results can be used to identify experimentally accessible diagnostics to yield fundamental insights.

During the past year, we explored the relationship between the spectrum of Lyapunov perturbation vectors and exponents with the pattern of the fluid convection. Using these Lyapunov diagnostics, we computed an estimate of the dimension describing the strange attractor in phase space called the fractal dimension. We compared this with the experimentally accessible Karhunen-Loeve dimension. The Karhunen-Loeve dimension was found to be 20 times larger than the fractal dimension for our values of the system parameters. We used Jazz to perform some of the numerical simulations used in these findings.

We also studied Rayleigh-Bénard convection in the turbulent regime and used Jazz for extensive convergence tests to ensure that these simulations accurately represent the system. We found that a large-scale circulation exists and its angle of orientation drifts with time, in good agreement with experiments. We also observed at least one probable cessation. We measured the dependence of heat transport on Rayleigh number; our scaling exponent of 0.30 ± 0.01 is in agreement with many experiments. We found that the thickness of the viscous boundary layer is less than the thermal boundary layer, as is theoretically predicted for our Prandtl number (0.4). These results shed new insight on the fundamental nature of the complex dynamics that occur in experimentally accessible fluid systems. Our findings can be used to improve our understanding of more complex real-world systems such as the dynamics of the weather and climate.

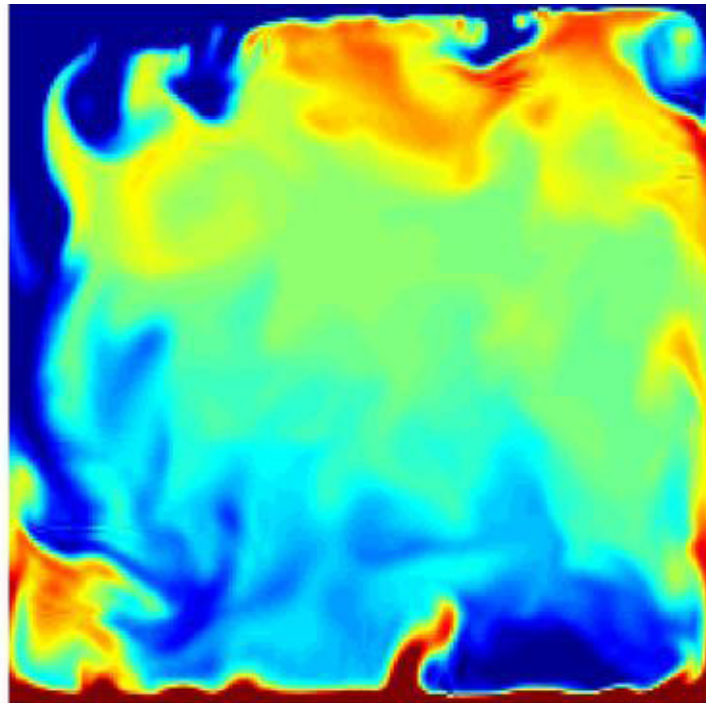


Figure 4: An x -constant (z versus y) color density plot of the temperature in the cell for a Rayleigh number of $1E8$, and a Prandtl number of 0.4 . One can see the counterclockwise large-scale circulation as well as the thermal plume creation in the top and bottom boundary layers. Also of interest are the backrolls in the upper right and lower left.

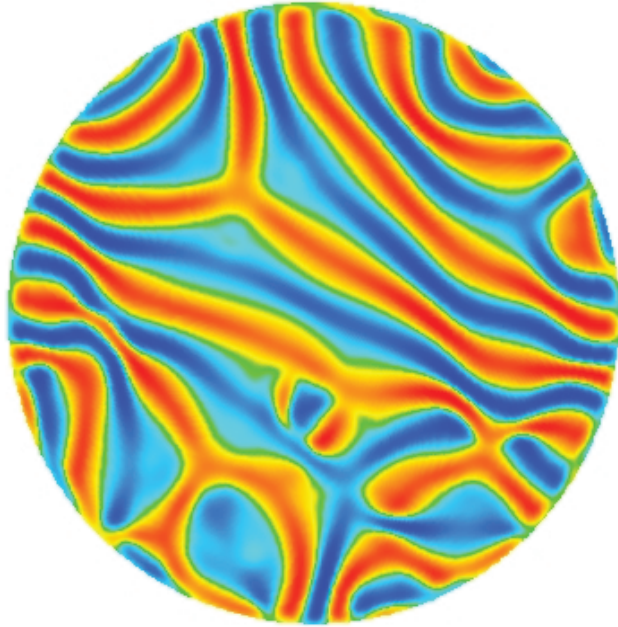


Figure 5: Typical pattern of convection rolls from a numerical simulation of chaotic Rayleigh-Benard convection in a shallow cylindrical domain. The flow field is shown at mid-depth; red indicates warm rising fluid and blue indicates cool falling fluid. For this simulation radius/depth = 10, the Rayleigh number is 3.5 times the critical value, and the Prandtl number is unity.

Publications and Presentations

A. Duggleby and M.R. Paul, The consequences of finite-time proper orthogonal decomposition for an extensively chaotic flow field, preprint, 2009.

M.R. Paul and A. Karimi, Extensive chaos in fluid convection, Presentation at *Dynamics Days Europe*, Göttingen, Germany, 2009.

M.R. Paul, Quantifying spatiotemporal chaos in Rayleigh-Benard convection, Presentation at the minisymposium on *Characterization of Spatiotemporal Chaos*, SIAM Conference on Applications of Dynamical Systems, for 2009.

J. Scheel, Go with the flow: Numerical simulations of turbulence in fluids, Presentation at the *Harvey Mudd Colloquium*, 2009.

J. Scheel, Go with the flow: Numerical simulations of turbulence in fluids, Presentation at the *Occidental College 2009 Summer Research Program Seminar Series*, 2009.

J. Scheel, P. Mutyaba, and T. Kimmel, Patterns in rotating Rayleigh-Benard convection at high rotation rates, Preprint, 2009.

J. Scheel and K. White, Turbulent thermal convection, Presentation at the *SIAM Conference on Applications of Dynamical Systems*, 2009.

Simulations of High Energy Collider Physics Processes

PIs: Edmond Berger (Physics)

Supersymmetry is the leading candidate for new high energy physics that goes beyond the Standard Model description of particle physics. This compelling theory predicts the existence of a significant number of new particles that should be observed at the CERN Large Hadron Collider (LHC). However, significant uncertainties exist in the current estimates of the supersymmetry processes themselves, as well as in the Standard Model backgrounds to many signatures of new physics.

To address these limitations, we conducted detailed numerical simulations of the distributions in phase space expected from both the new physics signal and several standard model backgrounds, searching for kinematic variables and distributions that would best serve as discriminators. We found that a potentially useful discriminant is the amount of “missing energy” produced. This missing energy is the energy carried away by essentially noninteracting final state particles, such as neutrinos. Nevertheless, the overall magnitude of the background is so large in our estimations that “tails” of the background extend well into the signal region, and more complex multivariable analysis strategies are needed (see Figure 6).

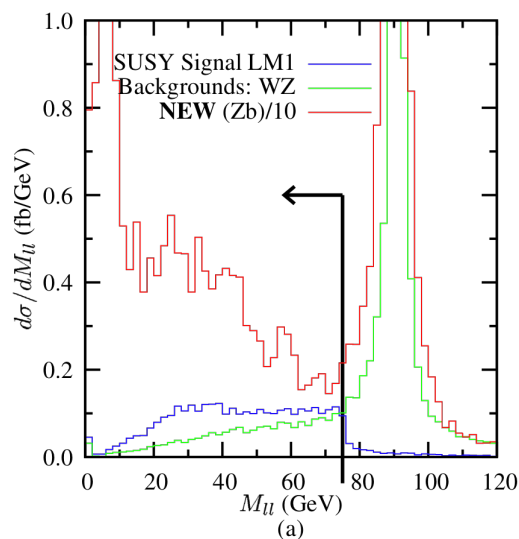


Figure 6: Collider processes.

Several technical challenges arise in simulating processes that may occur one time in a trillion. Each iteration must pass a battery of computationally expensive tests that simulate how a physical detector would respond. Since a brute-force approach is not feasible, we factorized the problem into stages that could be iteratively optimized to remove most of the samples that could not satisfy the final conditions. We also developed optimized algorithms to extract a dense set of results that were written to a newly optimized data format and postprocessed to allow for high-level analysis. The Jazz cluster’s ability to compress each CPU-months-long calculation into a few days proved essential for this research.

Coupled with previous work on two-lepton final states, the results of this new project confirm that the class of previously ignored heavy-flavor hadron decays will pose a serious challenge to the analysis of a wide range of experimental signatures. Given the complexity of the simulations, a

major experimental effort will be required to understand what in situ measures can be developed to quantitatively control the uncertainties.

Publications and Presentations

E. L. Berger and Z. Sullivan, Trilepton production at the CERN LHC: SUSY signals and Standard Model backgrounds, e-Print: arXiv:0909.2131 [hep-ph]. To be published in *Proceedings of Science*, proceedings of the European Physical Society Europhysics Conference on High Energy Physics - EPS-HEP 2009, Krakow, Poland, July 16–22, 2009.

E. Berger, **Dilepton and trilepton production – Standard Model and beyond the Standard Model**, Invited plenary talk, *Workshop on Higgs Boson Phenomenology*, ETH and University of Zürich, Switzerland, January 8, 2009.

E. Berger, Trilepton production at the CERN LHC: SUSY signals and Standard Model backgrounds, Presentation at the *2009 Europhysics Conference on High Energy Physics* July 16–22, 2009, Krakow, Poland.

E. Berger, Estimates of Standard Model backgrounds in searches for new physics – the case of isolated leptons, Presentation at the *Workshop on Searching for New Physics at the LHC*, Galileo Galilei Institute, Florence, Italy, September 8, 2009.

Density Functional Theory Calculations of Electrocatalytic and Nanocatalytic Phenomena

PIs: Jeffrey Greeley (Center for Nanoscale Materials)

The basic goal of this research is to use state-of-the-art electronic structure calculations, primarily density functional theory (DFT), combined with simple thermodynamic formalisms, to examine several systems of interest to the fuel cell and catalysis communities.

Much of our work this past year involved the computational analysis of oxygen reduction reaction (ORR) catalysts. Since the inefficient kinetics of the ORR is the primary limitation on the performance of low-temperature fuel cells, there is substantial interest both in developing fundamental understanding of the ORR on transition metal catalyst surfaces and in finding improved strategies to identify better ORR catalysts. Using intensive DFT calculations, we assessed the suitability of over 700 binary metal alloys for ORR performance. Our results predict that one such alloy, a mixture of silver and palladium, has properties superior to those of platinum, the canonical ORR catalyst; this prediction is being tested experimentally. We also demonstrated a new, fundamental effect in the control of ORR-based surface properties. We showed that, in contrast to widely held intuition, solvated cations near the catalyst surface can dramatically affect the activity of ORR catalysts. This effect, confirmed with careful experimental studies, may be a useful strategy for tuning catalytic activity in fuel cells.

We also obtained important results concerning the effect of magnetism on the catalytic properties of subnanometer metal clusters. The calculations on Jazz demonstrate a pronounced change in the

activation barrier of both the methanation reaction (where methane is produced from a feed stream of carbon monoxide and hydrogen in a high-temperature process) and the dissociation of methyl nitrate (where methoxy and nitrogen oxide are produced in a low-temperature catalytic process). On four-atom nickel, cobalt, and iron clusters, each of these reactions was found to proceed at significantly higher rates on nonmagnetized clusters than on fully spin-optimized clusters. These results strongly suggest that magnetic-nonmagnetic transitions might lead to measurable changes in catalytic rates on small metal clusters. Careful manipulation of these transitions might serve as an additional “tuning knob” for catalytic properties.

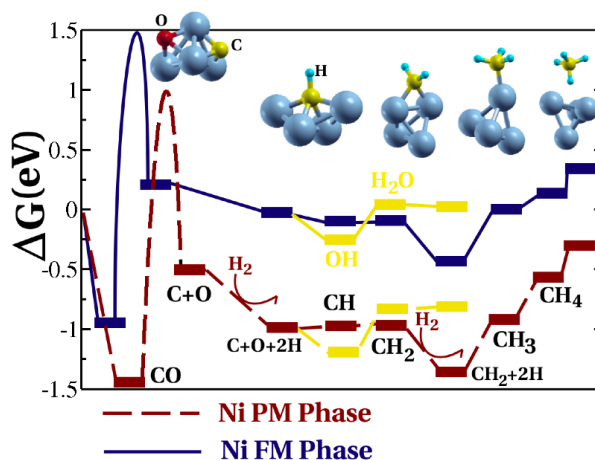


Figure 7: Calculated free energies of methane formation from CO and H₂ on Ni₄ clusters in both magnetized and nonmagnetized states. The magnetic transition causes significant changes in the reaction free energies.

Publications and Presentations

J. Greeley and J. K. Nørskov, Combinatorial density functional theory-based screening of surface alloys for the oxygen reduction reaction, *J. Phys. Chem. C*, **113** (2009) 4932.

C. A. Lucas, P. Thompson, M. Cormack, A. Brownrigg, B. Fowler, D. Strmcnik, V. Stamenkovic, J. Greeley, A. Menzel, H. You, and N. M. Markovic, Temperature-induced ordering and phase transitions in metal/adsorbate structures at electrochemical interfaces, *J. Am. Chem. Soc.*, **131** (2009) 7654.

S. Vajda, M. J. Pellin, J. Greeley, C. Marshall, L. A. Curtiss, G. A. Ballentine, J. Elam, S. Catillon-Mucheri, P. C. Redfern, and P. Zapol, Subnanometer platinum clusters: Highly active and selective catalysts for oxidative dehydrogenation, *Nature Materials*, **8** (2009) 213.

D. Strmcnik, K. Kodama, D. van der Vliet, J. Greeley, V. R. Stamenkovic, and N.M. Markovic, The role of non-covalent interactions in electrocatalytic fuel-cell reactions on platinum, *Nature Chemistry*, **1** (2009) 466.

J. Greeley, F. Mehmood, and L. Curtiss, Density functional studies of methanol decomposition on subnanometer Pd clusters, preprint, 2009.

DFT Screening Investigation of Catalytic and Electrocatalytic Phenomena of Transition Metals

PI: Rees Rankin (Center for Nanoscale Materials)

It is well known that H_2O_2 historically has not been synthesized efficiently by direct conversion of H_2 and O_2 . Recent work in the literature suggests metallic alloy nanoparticles can create new chemistry in the selective synthesis of H_2O_2 from H_2 and O_2 . In 2009, we focused on the characterization of reaction mechanisms and energetic for the selective formation of H_2O_2 on transition metal (TM) surfaces using first-principles based on extensive DFT calculations. We performed electronic structure calculations, combined with simple thermodynamic formalisms, to characterize the geometry and energy of the various intermediates and products in this reaction on ideal close-packed surfaces of unitary TM species (including Ag, Au, Co, Cu, Fe, Ir, Ni, Os, Pd, Pt, Rh, and Ru). Based on results from these initial calculations, we began performing additional calculations on step surfaces, alloy surfaces, and skin surfaces from the most promising TM species identified in the initial calculations. We analyzed our data through Sabatier volcano diagrams to identify the most promising species for alloying to improve catalytic rate and selectivity. The results suggest that H_2O_2 selective synthesis on TM-based surfaces requires optimization of competing effects that dominate the reactivity and selectivity via binding effects in both H and O species to the surface. The most promising TM species identified near the top of our Sabatier volcano include Pd and Au, as well as 3-4 other TM species. Based on our results, we will work toward a screening-based prediction of the most optimal binary (or ternary +) TM catalysts for H_2O_2 selective synthesis.

The development of our methodology for the H_2O_2 reaction mechanism fits into a broader goal of building a large database of computationally derived properties of catalysts and catalytic reactions. This broad database will accelerate materials-by-design screening of catalytic materials and reactions through pretabulated data. The results of our research will also provide insight into intermediate and product species, as well as reaction mechanisms and energies that may be present in various oxygen reduction reaction scenarios.

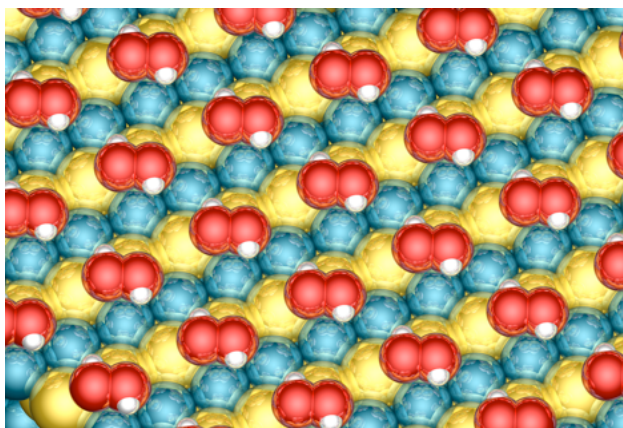


Figure 8: *Depiction of a low coverage ($\frac{1}{4}$ ML) of H_2O_2 adsorbed in a minimum energy geometry state on one possible near-surface Pd-Au skinned Pd(111) substrate. The binding geometry in this adsorbate complex is essentially identical to that on the pure Pd(111) and Au(111) surfaces.*

Publications and Presentations

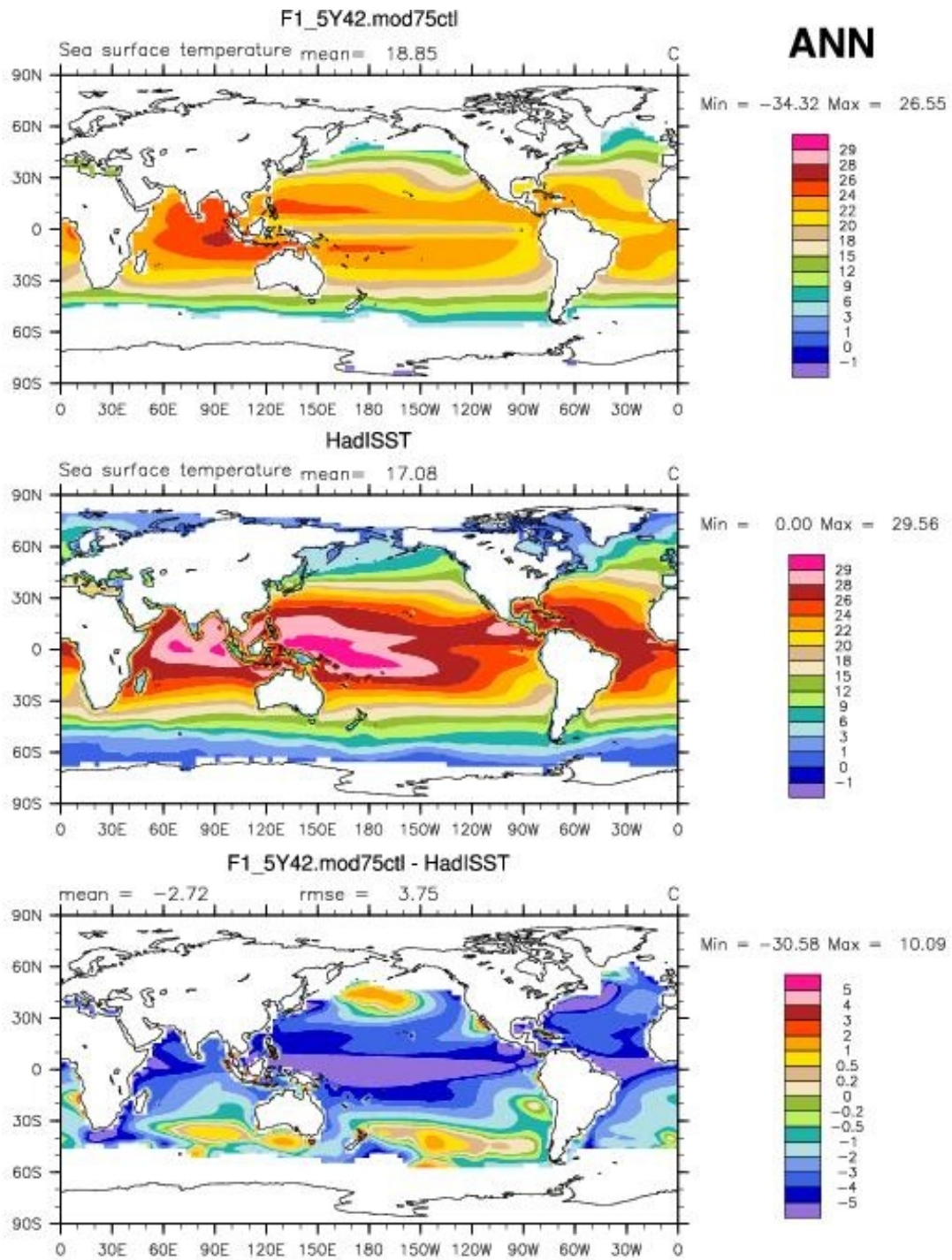
R. Rankin and J. Greeley, Presentation at the *AICHE annual meeting*, 2009.

Global Climate Modeling with the Fast Ocean Atmosphere Model

PI: Robert Jacob (Mathematics and Computer Science Division)

The goal of the FOAM project is to maintain a fully coupled climate model that puts an emphasis on high throughput as measured in simulated years per day. Like most climate models, FOAM is composed of separately developed pieces, many developed by other groups. The atmosphere model, PCCM3, contains two numerical methods: a spectral transform scheme for the dry dynamics and a semi-Lagrangian transport scheme for moisture. Both methods have been parallelized with a two-dimensional decomposition of the horizontal dimension. The physics, which refers to all the parameterizations of phenomena such as radiation and convection, is done entirely within a vertical column and so parallelizes trivially with the dynamics. The ocean model, Om3, uses a finite-difference method with explicit subcycled time stepping; it also has a 2D parallel data decomposition and does the small amount of ocean physics in columns. The other pieces of FOAM include a land model (which contains no dynamics and can be thought of as an extension of the atmosphere column physics) and a sea ice model. These pieces are integrated into a single system with a special-purpose coupler.

During 2009 we worked on raising the horizontal resolution in Om3 from 1.4 degrees to approximately 1/6 of a degree—high enough to resolve the eddy scale in the ocean. The reason for doing this work is that eddies transport heat and momentum in the ocean and, if they are not resolved explicitly, they must be parameterized—something that is often done poorly. An eddy-permitting model, coupled to a high-resolution atmosphere model, can be a better tool for estimating changes in heat transport caused by global warming. We carried out several successful test integrations on Jazz to determine the next step in adjusting some of the parameters of the model. This project is expected to lead to a new, high-resolution coupled ocean-atmosphere model that will be an important addition to the small family of such models (see Figure 9).



Created: Fri Jul 30 09:00:28 CDT 2004

DIAG Version: 030429

Figure 9: North Atlantic sea surface temperature from year 6 of a 10-year test integration. The Gulf Stream is not separating at the correct place and creating a large gyre off the U.S. East Coast. We are investigating the reasons.

HEIGHTS-3D Modeling

PI: Tatyana Sizyuk (Mathematics and Computer Science)

The HEIGHTS team has developed comprehensive and integrated models in multidimensional geometry (see Figure 10). Using the HEIGHTS suite, we studied the response of plasma-facing components to energy deposition at edge-localized modes (ELMs), disruptions in fusion devices, and runaway electrons in real tokamak reactor geometry. Our simulation results show that disruptions and high-power ELMs cause excessive target erosion of candidate materials and possible plasma contamination. The long-term impact can cause melting of structure and burnout of coolant tubes. For example, runaway electrons penetrate deeply into the first wall with a beryllium coating and result in melting and damage of the beryllium/copper interface. On the other hand, using a tungsten coating for the first wall protects the structural material, but the tungsten armor suffers significant melting and splashing.

We also updated several parts of the HEIGHTS package and added new components. For example, a 3-D model for runaway electrons energy deposition in real geometry is a new, parallelized code.

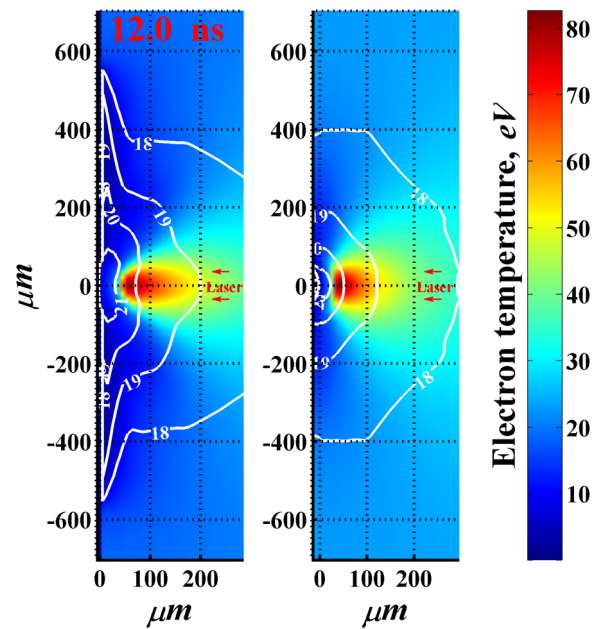


Figure 10: HEIGTS results for the effects of plasma spatial profile on conversion efficiency of laser-produced plasma sources for extreme ultraviolet lithography. Electron temperature and density (white contours) distributions in planar (left) and droplet (right) target geometries.

Publications and Presentations

A. Hassanein, T. Sizyuk, and I. Konkashbaev, Integrated simulation of plasma surface interaction during edge localized modes and disruptions: Self-consistent approach, *J. Nucl. Mater.*, **390–391** (2009) 777–780.

A. Hassanein, V. Sizyuk, T. Sizyuk, and S. Harilal, Effect of plasma spatial profile on conversion efficiency of laser produced plasma sources for EUV lithography,” *J. Micro/Nanolith. MEMS MOEMS*, **8** (Oct. 2, 2009) 041503.

V. Sizyuk and A. Hassanein, Self-consistent analysis of the effect of runaway electrons on plasma facing components in ITER, *Nucl. Fusion*, **49** (2009) 095003.

Mechanisms of CO Hydrogenation by Homogeneous Cobalt Catalysts

PIs: Larry Curtiss (Materials Science) and Randall Meyer (University of Illinois at Chicago)

We are using the VASP (Vienna Ab Initio Simulation Package) code to investigate the hydroformylation of propene or ethylene with cobalt-based homogeneous catalysts. Researchers in the Chemical Engineering Division at Argonne have generated experimental data regarding the performance of these catalysts, but many unanswered questions remain about the precise mechanisms and intermediates involved. Our aim is to test various hypotheses for the mechanisms in an effort to understand how to improve catalyst selectivity.

During the past year we focused on the mechanisms of methanol, methyl formate, and ethylene glycol formation using cobalt carbonyl catalysts. The complete reaction pathway has now been determined. We found that the product selectivity can be explained by the relatively low barrier for formation of the methoxy intermediate (0.32 eV) vs. the hydroxymethyl intermediate (0.73 eV).

Hydrogenation

PIs: Randall Meyer (University of Illinois at Chicago) and Jeffrey Miller (Chemical Sciences and Engineering)

Our goal is to understand the effect of particle size on the electronic structure of small metal nanoparticles. While it is well known that the decreased coordination of surface atoms in metal particles makes them more reactive, interpretation of experimental results that correlate structure and reactivity is not always straightforward. Generally, the size of the “white line” in spectra from X-ray Absorption Near Edge Spectroscopy (XANES) is believed to be related to the number of unoccupied orbitals into which electron ejected from the core can scatter if the selection rule of $\ell = \pm 1$ is satisfied.

To investigate this phenomenon, we examined the change in electronic structure of Pt clusters of 1-6, 13, and 55 atoms, over varying catalytic supports (SiO_2 , Al_2O_3 , C, $\text{SiO}_2\text{-Al}_2\text{O}_3$, TiO_2). Density functional theory calculations were performed to aid in the analysis of electronic structure and to establish relationships between the density of states and the white-line intensity in the XANES spectra. We observed (as expected) that the center of the *d*-band of Pt clusters shifts toward the Fermi level as the particle size decreases. In addition, we noticed that the density of state narrows both above and below the Fermi edge. We also reproduced the experimentally

observed bond contraction as the particle size shrinks, and we noticed an increase in the hybridization of d -electrons occurs, leading to an increase in the white intensity. Similarly, we calculated the density of states for CO/Pt(111) and Pt₁₃(CO)₁₂ and observed a complete loss of d -electron density in surface Pt atoms when CO is adsorbed. We do not view this as charge transfer creating “ d -holes” that are now available to an ejected photoelectron. Rather, we interpret our results as showing the creation of new bonding and antibonding orbitals that are below and above the edge, respectively. These antibonding orbitals lead to the creation of new orbitals that must have some “ d -character” allowing the transition from the $2p$ core orbital. Our results suggest a new interpretation of XANES data that, if correct, represents a huge step forward for our understanding of the electronic structure of metal nanoparticles and the bonding of adsorbates to surfaces (see Figure 11).

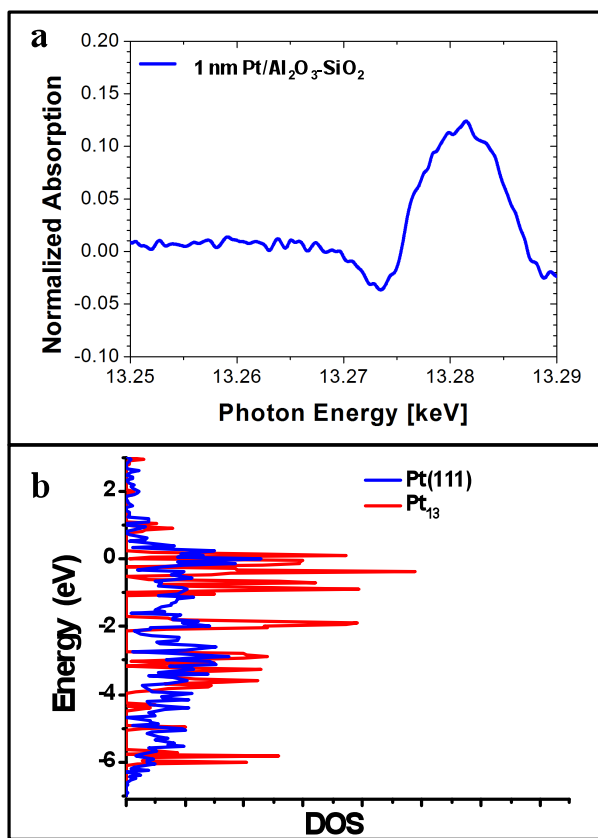


Figure 11: Correlating XANES and DOS calculations: (a) difference spectra between a 1 nm Pt/Al₂O₃-SiO₂ catalyst and Pt foil at the L_{II} edge; (b) DOS calculation comparing a Pt₁₃ cluster and a Pt(111) slab.

Publications and Presentations

R. Meyer, Y. Lei, J. Miller, Trends in X-ray absorption near edge spectroscopy of supported Pt nanoparticles, presentation, 21st Meeting of the North American Catalysis Society, San Francisco, June 7–12, 2009.

Studies of Voltage-Gated Potassium Channels

PIs: Benoit Roux and Yuqing Deng (Biosciences)

Voltage-gated potassium (Kv) channels are membrane proteins that respond to changes in the transmembrane potential by altering their conformation to allow the passive conduction of K⁺ ions across the cell membrane. Upon depolarization of the membrane, the voltage-sensing domain in each subunit undergoes a voltage-dependent transition from a resting to an active conformation, which then leads to the opening of the intracellular gate of the ion conduction pore. Ultimately, explaining the voltage-gating mechanism of Kv channels in molecular terms requires gaining knowledge of the active and resting conformations and then showing how those conformations are able to account for the experimentally observed gating charge. Our goal is to refine the atomic models of the closed/resting and open/activated states and test their ability to account for the experimentally observed gating charge. For this effort, we are using all-atom molecular dynamics techniques.

During the past year we conducted simulations of membrane proteins and the binding free energy of ligands, developed polarizable models of membranes and reverse osmosis membranes, and formulated methods to compute large conformational changes. One of our most exciting projects has been the simulation of a polymerized membrane used to perform reverse osmosis, a process used for desalinating seawater (see Figure 12). We constructed the first atomistic model of such a membrane and then calculated the rate of permeation of water molecules through the membrane. The results were in good agreement with experimental estimates (which are fairly uncertain). This project paves the way for using detailed atomic models and computer simulations in future efforts aimed at designing and improving materials in technological applications.

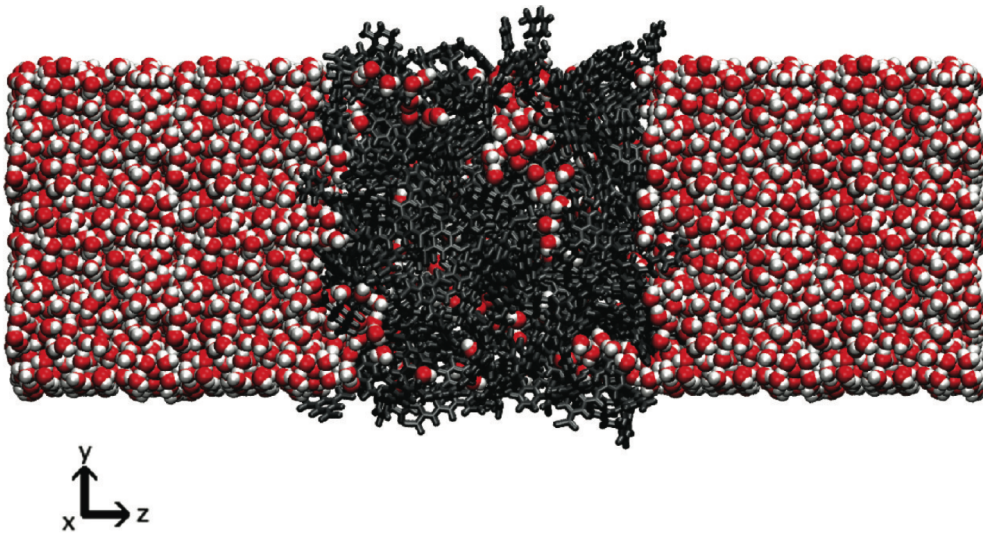


Figure 12: Configuration for the simulation of water with the polymer membrane. Molecular dynamics (MD) simulations were used to investigate the properties of an atomic model of an aromatic polyamide reverse osmosis membrane. The monomers forming the polymeric membrane are cross-linked progressively on the basis of a heuristic distance criterion during MD simulations until the system interconnectivity reaches completion. Equilibrium MD simulations of the hydrated membrane are then used to determine the density and diffusivity of water within the membrane. Given a 3 MPa pressure differential and a 0.125 μm width membrane, the simulated water flux is calculated to be 1.4×10^{-6} m/s, which is in good agreement with an experimental flux measurement of 7.7×10^{-6} m/s. Taken from Harder et al. (2009).

Publications and Presentations

Y. Deng, and B. Roux, Computations of standard binding free energies with molecular dynamics simulations, *J. Phys. Chem. B*, **113** (2009) 2234–2246.

E. Harder, A. D. Mackerell, and B. Roux, Many-body polarization effects and the membrane dipole potential, *J. Am. Chem. Soc.*, **131** (2009) 2760–2761.

E. Harder, D. E. Walters, Y. D. Bodnar, R. S. Faibish, and B. Roux, Molecular dynamics study of a polymeric reverse osmosis membrane, *J. Phys. Chem. B*, **113** (2009) 10177–10182, 2009.

S. Park, J. P. Bardhan, B. Roux, and L. Makowski, Simulated X-ray scattering of protein solutions using explicit-solvent models, *J. Chem. Phys.*, **130** (2009) 134114.

S. Yang, S. Park, L. Makowski, and B. Roux, A rapid coarse residue-based computational method for x-ray solution scattering characterization of protein folds and multiple conformational states of large protein complexes, *Biophys. J.*, **96** (2009) 4449–4463.

Lattice Quantum Chromodynamics

PI: Don Sinclair (High Energy Physics)

Relativistic heavy-ion collisions can produce hot nuclear matter. At low temperatures this is a solid or liquid composed of hadrons. At high temperatures it becomes a liquid or gas composed of quarks and gluons, the so-called quark-gluon plasma. We have been studying the transition between nuclear matter and the quark-gluon plasma, which can be observed in relativistic heavy-ion colliders. For these studies, we use lattice quantum chromodynamics (QCD).

At present we are performing simulations designed to yield an approximate equation of state for such hot nuclear matter. Specifically, we carry out numerical integration of the equations of motion that describe QCD dynamics on a discrete space-time lattice. The inclusion of a stochastic driving term distributes the equilibrated fields according to the grand-canonical ensemble. The simulation method we use is called the rational hybrid Monte Carlo algorithm (see Figure 13).

To calculate the equation of state, we need to simulate over a range of temperatures and chemical potentials. Because of the large number of simulations required, we spread our calculations over several computer systems, one of which was Jazz. Jazz has the advantage that small (in terms of numbers of processors) jobs are not discriminated against, as they are on some other systems. We also used Jazz to perform all of the associated zero temperature, zero chemical potential simulations that are required to yield subtractions needed to extract pressure and energy densities from our finite temperature measurements.

We plan to compare our calculated equation of state to that obtained by others using series expansions in terms of chemical potential, and possibly to other approximation methods such as the resonant hadron-gas model. We hope this work will further our knowledge of the physics of relativistic heavy-ion collisions.

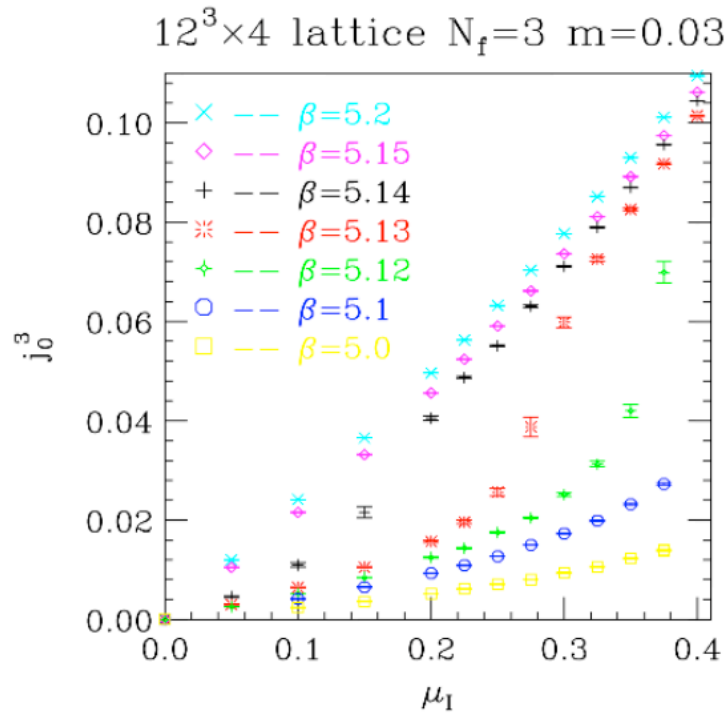


Figure 13: *Quark-number densities as functions of chemical potential (μ) for various choices of $\beta = 6/g^2$. These are proportional to $dp/d\mu$, where p is pressure.*

Lithium-Ion Battery Electrode Modeling

PI: Roy Benedek (Physics)

We are simulating the physical and electrochemical properties of proposed electrode materials for lithium batteries. Our aim is to characterize the adhesion of different coatings to the electrode, dissolution of the electrode in acid, the transport of lithium ions in the vicinity of electrode interfaces, and the ability of dopants near the interface to protect the electrode against dissolution. This work complements an experimental program in the Battery Department of Argonne's Chemical Sciences and Engineering Division).

One promising electrode material for lithium-ion batteries is lithium manganese spinel (LiMn_2O_4). Although the bulk behavior of this material is relatively well understood, surfaces, interfaces (with moisture, organic electrolyte, or protective coatings), and the structure of nanoscale particles are poorly characterized. Electrode interfaces, however, are crucial for the reactions that enable a battery to function. In recent work on Jazz, we performed first-principles density functional theory simulations on a small stoichiometric spinel particle in vacuum, with eight formula units (56 atoms), to gain insight into atomic structure and chemical bonding of such a cluster. The structure was allowed to relax by first-principles molecular dynamics at room temperature and by conjugate gradient relaxation, to determine the optimal structure for such an

atomic cluster. The positions of the three most poorly bonded Mn atoms, located on cube edges in the initial structure, along with neighboring oxygen atoms, rearranged to form dendritelike structures projecting out of the cube (Figure 14). The Mn-O bond lengths decrease significantly to compensate for the coordination deficit of the edge Mn atoms. A rough estimate indicates that the surface energy of the cluster is of order 1 J/m^2 , the expected order of magnitude.

The next step is to apply coating materials, particularly oxides, to the cluster, in order to determine their adhesion and their ability to transport lithium atoms through the coating and into the spinel electrode. We will also investigate the influence of delithiation (charging) of the spinel cluster on the atomic structure.

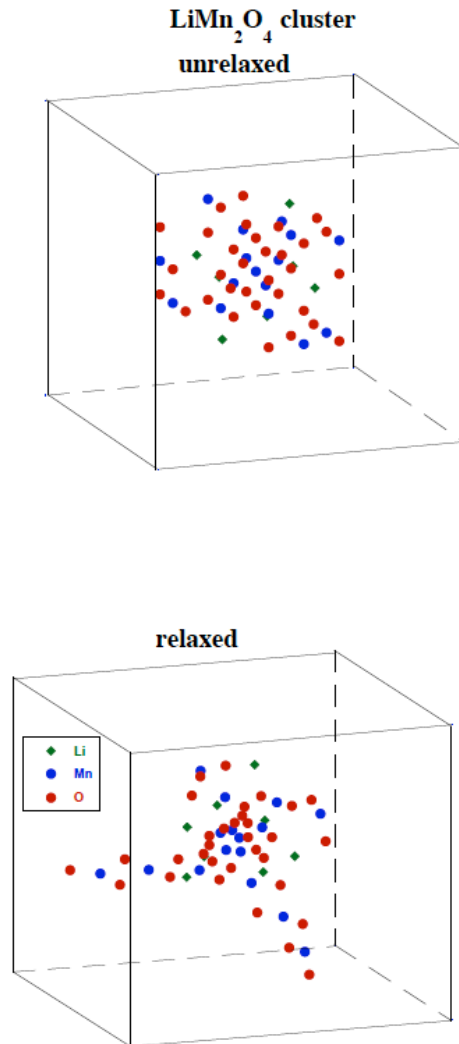


Figure 14: Atomic configuration of the LiMn₂O₄ cluster before relaxation (above) and after relaxation (below). This illustrates two of the three (the third is masked by the core of the cluster) dendritelike structures protruding from the cluster, which result from oxygen atoms compensating for the low coordination of the three Mn atoms located on cube edges.

Monte Carlo Characterization of Accelerator-Driven Subcritical Facilities

PI: Yousry Gohar (Nuclear Engineering)

YALINA Booster subcritical assembly was constructed to examine the physics of Accelerator Driven Systems (ADS). The subcritical assembly is driven by an external neutron source. It consists of four concentric square zones: a target zone, an inner fast zone, an outer fast zone, and a thermal zone without an active cooling system. The inner fast zone utilizes high enriched metallic uranium fuel rods with 90% ^{235}U , the outer fast zone contains uranium oxide fuel rods with 36% ^{235}U , and the thermal zone uses uranium oxide fuel rods with 10% ^{235}U (EK-10 fuel type). In-between the outer fast and the thermal zones, a thermal neutron absorber zone is used. The absorber zone allows fast neutrons to stream from the fast zone to the thermal zone and diminish the opposite streaming of thermal neutrons. The assembly is surrounded by a radial graphite reflector. At the ends of all fuels rods, borated polyethylene reflector is used. The subcritical assembly has ten experimental channels and six measurement channels.

Argonne National Laboratory examined the replacement of the high enriched uranium (HEU) fuel of YALINA Booster subcritical assembly with low enriched uranium (LEU) fuel without penalizing its performance. Analytical analyses have been performed based on the use of Monte Carlo and Deterministic methods. MCNPX, MCB, MONK, and ERANOS computer codes with different nuclear data libraries based on ENDF-B/VI, -VII, and JEF3.1 have been employed for static and kinetic analyses. The geometrical details are included explicitly without approximation or homogenization in the Monte Carlo models. In the experimental program, the subcriticality has been measured as a function of the number of the fuel rods loaded in the subcritical assembly. Different methods have been used to measure the assembly subcriticality, the spatial neutron flux distribution, spectral indices, and transmutation reactions rates.

The ERANOS analytical results of the multiplication factor with JEF3.1 nuclear data files agree with the experimental results with a maximum difference of 50 pcm for the original configuration with 1141 EK-10 fuel rods in the thermal zone. The use of ENDF/B-VI.8 instead of JEF3.1 reduces the multiplication factor by 80 pcm. The K_{src} calculation results are higher than the effective multiplication. Time dependent studies with KIN3D module of ERANOS have been performed to calculate the helium detector response from D-D and D-T pulse neutron sources and it is compared with the experimental results as shown in Fig. 1a. Monte Carlo analyses have been performed with MCNPX computer code using JEF3.1 and ENDF/B-VI.6. An example of the comparison between the experimental measurements and the calculated values is shown in Figure 15b.

The booster zone of the original YALINA-Booster configuration has 695 fuel rods (132 90% and 563 36%) with high enriched uranium. These 695 fuel rods have been replaced with 651 fuel rods with 21% enriched uranium, which leaves some empty fuel cells in the booster zone. In addition, all the available inventory of EK-10 fuel rods, which is 1185 rods, has been used in the thermal zone of the YALINA-Booster. The resulting configuration has a neutron multiplication of ~ 0.95 . A parametric study has been carried out to reconfigure the absorber zone to achieve a subcriticality level around 0.98 without reconstructing the assembly. The obtained configuration is shown in Fig. 16a with a neutron multiplication factor of ~ 0.98 . The neutron flux calculation shows that the spatial distribution is similar to the distribution of the original configuration. In the new configuration, the absorber zone has a circular arrangement instead of a square. Figure 16b shows the total neutron flux map of the new configuration due to a D-T neutron source.

YALINA-Booster subcritical assembly have been successfully modeled and the comparison between the analytical results and the experimental measurements shows excellent agreement. The original assembly has been reconfigured to use low enriched uranium instead of the high enriched uranium without penalizing the original performance. The comparison and the conversion analyses were done for the first time ever using a high fidelity computational method. The JAZZ cluster provided the computational resources.

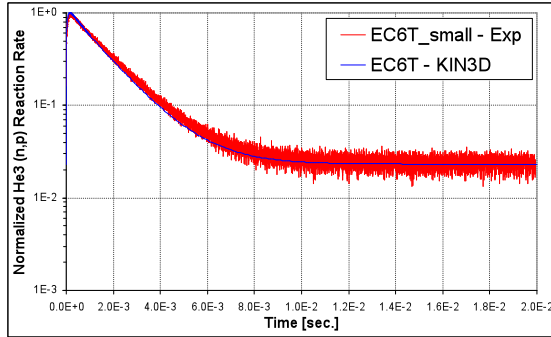


Fig. 15a: Experimental measurements and ERANOS analytical simulation results of He-3 detector response comparison located at the center of the EC6T experimental channel of the YALINA-Booster original configuration due to pulsed D-D external neutron source at the assembly center.

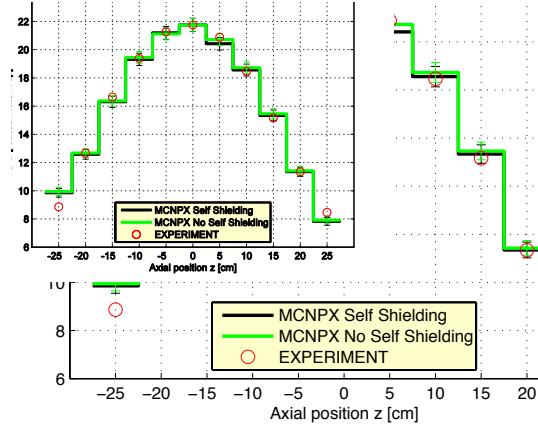


Fig. 15b: Experimental measurements and MCNPX analytical simulation results of He-3 detector response comparison along the EC6T experimental channel due to Cf external neutron source located at the assembly center.

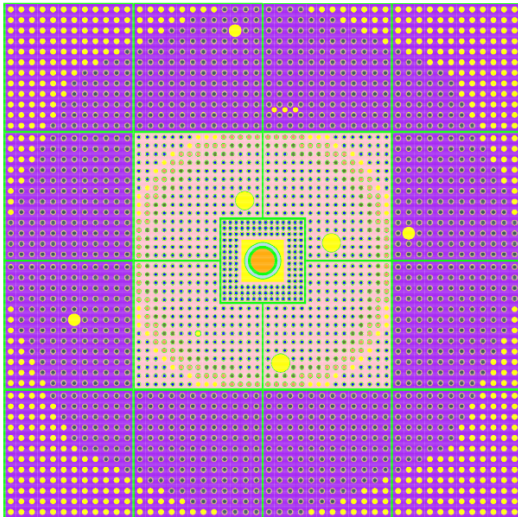


Fig. 16a: Horizontal section of MCNPX geometrical model of YALINA-Booster configuration with 21% enriched fuel rods in the booster zone shown without the graphite reflector.

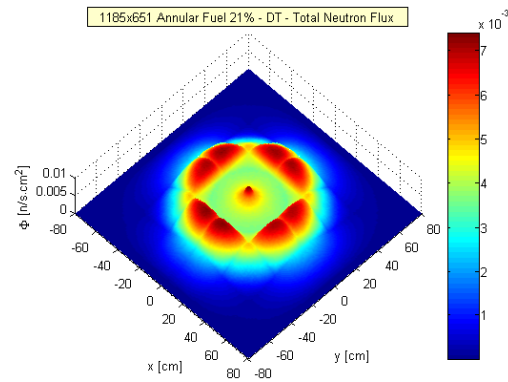


Fig. 16b: Total neutron flux map of the YALINA-Booster configuration with 21% enriched fuel rods in the Booster zone due to a D-T neutron source at the assembly center.

Energy Production from Spent Nuclear Fuels and Transmutation of Long-Lived Fission Products

PI: Yousry Gohar (Nuclear Engineering)

The neutron rich Tokamak fusion devices are very attractive to transmute the Minor Actinides (MA) of the spent nuclear fuel and produce energy. The high energy neutrons of the Deuterium–Tritium fusion fuel cycle enhance the transmuter neutron economy through neutron multiplication and extra neutrons per fission reaction. Over the years, subcritical Fusion-Fission Hybrid Systems (FFHS) have been proposed for fissile breeding, energy production, and dispose of spent nuclear fuel. Recently, FFHS have been reconsidered to close the nuclear fuel cycle of the fission power reactors. Different concepts have been examined to fission the MA, to produce energy from the fission process, to minimize the required geological storage capacity, and to close the fission reactor fuel cycle. Most of the concepts avoid slowing down the neutrons to enhance the FFHS performance. Both stationary and mobile nuclear fuel forms have been examined in these concepts. In this work, a mobile fuel is considered because of the desire to minimize the number of the fuel processing steps and to avoid storing the irradiated nuclear fuels. Both the molten salts and Li-Pb eutectic are considered as the carriers for the transuranics. The use of the Li-Pb eutectic results in a fast neutron spectrum, which is preferred for MA incineration. This work examines a fusion fission concept utilizing the current fusion technologies with minimum extrapolation to incinerate the MA of the USA spent fuel inventory expected by 2015. The Li-Pb eutectic is utilized as the fuel carrier and coolant to maintain a hard neutron spectrum in the MA transmutation zone.

In this concept, the nuclear fuels are fabricated into TRISO-like fuel particles and mixed with the Li-Pb eutectic. The fuel particle density is adjusted to be the same as the Li-Pb eutectic, by adding lighter materials on the outer particle surface, i.e. carbon coating to form homogeneous slurry.

A Monte Carlo model for MCNPX is setup to simulate the neutron physics and the fuel transmutation of this FFHS concept. The blanket consists of a 0.5 cm thick First Wall (FW), a 60-cm fission zone, and a 100-cm graphite reflector. A uniform volume neutron source with a radius of 140 cm is used to drive the fusion fission blanket. The neutron wall loading is 0.1-MW/m². The neutron cross section library is generated from the ENDF/B-VII nuclear data files. The minor actinide fuel compositions are based on the processed PWR spent fuel, with 33GWd/MT burnup and 99.995% of uranium removed.

To define the fuel compositions of the FFHS system, fuel compositions with different plutonium percentages are considered. The first composition has no plutonium and the other compositions have different percentages of the spent fuel plutonium.

Figure 17 shows that the required fusion neutron power for generating 3 GW_t (~1 GW_e) is not sensitive to the fuel compositions, but is mainly determined by the neutron multiplication of the fission blanket. Its k_{eff} should be no less than 0.90 to require less than 30 MW fusion neutron power. The current fusion devices are operated in such power range only for short time. The extra requirement is to operate FFHS in steady state mode as much as possible to maintain the electric production. To generate 3GW_t fission power with a 12.5 MW fusion neutrons, a neutron multiplication factor of ~0.97 is required.

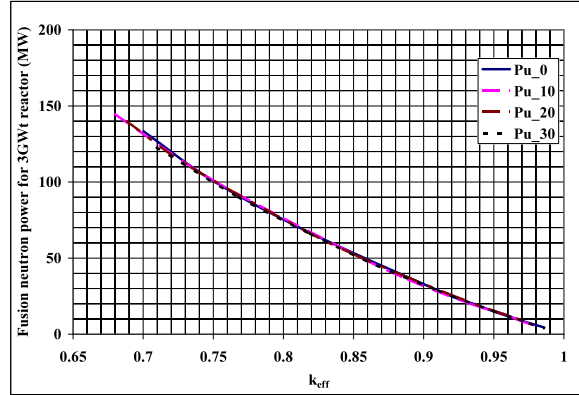


Figure 17: The required fusion neutron power for generating 3-GW_t as a function of the neutron multiplication factor.

The volume fraction of the fuel particles in the slurry is adjusted to achieve the different multiplication factors. Figure 18 shows the required fuel volume fraction to obtain k_{eff} of ~ 0.97 for each fuel composition for fusion device with 0.1-MW/m² neutron wall loading. The 94.4% plutonium loading represents the processed spent fuel without removing any plutonium. To support a 3GWt system with k_{eff} of ~ 0.97 and 0% plutonium concentration, the homogeneous slurry should have 28% by volume solid fuel particles, and the total actinides in the system are about 160 tons. With 30% plutonium concentration, the solid fuel volume percentage is reduced to 10.5% and it only requires about 62 tons of MA.

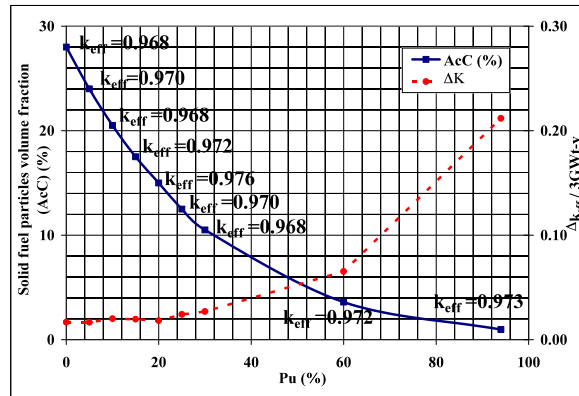


Figure 18: The volume percentage of the solid fuel particles in the slurry and the k_{eff} change after 3GWt-y burnup as a function of the plutonium loadings in the solid fuel.

For the case with 30% plutonium loaded in the solid fuel particles, the first wall radiation damage parameters are 15 dpa/FPY for the atomic displacement and 17 appm/FPY for the helium generation, which are low values relative to the expected parameters of a fusion power reactor. The fusion-fission blanket with Li-Pb Eutectic breeds enough tritium for fueling the plasma operation. In addition, the large neutron leakage from the blanket to the reflector can be utilized to breed additional tritium.

The MCB burnup computer code is utilized to simulate the MA transmutation in the FFHS with a fixed fission power, different fuel compositions corresponding to initial k_{eff} of ~ 0.97 . Figure 18

shows that loading a small amount of plutonium in the FFHS system, up to 30%, does not result in additional k_{eff} change relative to the 0% plutonium composition. After one full power, the k_{eff} value decreases by about 1700 pcm with 0% plutonium. If the processed fuel is directly used, the k_{eff} value decreases by more than 20000 pcm. Therefore, according to Fig.1, to maintain the 3GW_t power level at the end of the full power year, the fusion power has to be 1.5~2 times of the initial power for the case with 0% plutonium, but about 10 times for the case with 94.4% plutonium.

The fuel burnup in the FFHS system is tabulated in Table I after one full power year as a function of the plutonium loading. For each case, about 1.2 ton of MA and plutonium are burned in total. The total amount of MA transmuted decreases as more plutonium included in the fuel, so as the initial loading of MA. The USA MA inventory is ~ 40 tons from the 70,000 tons of USA spent nuclear fuel expected by 2015. Thus, loading a small amount of plutonium in the FFHS improves the annual transmutation of MA per ton (column 5 of Table I) of loaded fuel; however, the burned mass of MA with the same fission power is reduced (column 4 of Table I).

This work shows a possible Fusion-Fission Hybrid System, which can use the current fusion technologies to burn MA effectively. The fuel form is based on the developed technology of the TRISO fuel particles, which reduces the required development of new fuel form. The Monte Carlo simulations show that loading a small amount of plutonium into the system reduces the solid fuel particles in the fuel carrier dramatically. The preliminary burnup calculations also show that a small amount of plutonium in the system will not increase the reactivity swing significantly relative to the case without plutonium. In addition, the MA transmutation rate per ton of the initial loaded MA fuel is improved. The other main point is that the limited MA inventory requires loading fissile material to achieve and maintain the desired neutron multiplication of the FFHS. Additional work is underway to determine the limits and the optimal values for each of the system parameters and refueling scheme during the reactor lifetime.

Plutonium %	Total Incineration U+Np+Pu+Am +Cm/3GWt (ton)	Mass Change of U+Np+Pu /3GWt (ton)	Mass Change of Am+Cm /3GWt (ton)	Am+Cm/ton of the loaded MA fuel inventory (ton)
0	-1.15	1.69	-2.84	-0.018
5	-1.15	1.33	-2.48	-0.019
10	-1.18	1.02	-2.19	-0.021
15	-1.18	0.728	-1.91	-0.023
20	-1.19	0.437	-1.63	-0.030
25	-1.20	0.260	-1.46	-0.028
30	-1.19	0.077	-1.27	-0.029
60	-1.20	-0.73	-0.472	---
94.4	-1.17	-1.18	0.0072	---

Table I. FFHS burnup results for a 3GW_t after one full power year.

Coarse-Graining Methods for Molecular Dynamics and Their Application to Ion-Channel Proteins

PI: Jaydeep Bardhan (Mathematics and Computer Science)

We are investigating approaches for ensuring that molecular-dynamics (MD) simulations of biological systems faithfully reproduce experimental data. Model validation is critical if such simulations are to be trusted in making predictions for experimental verification. Until very recently, however, computational limitations prevented the scientific community from checking MD against a wide range of experimental measurements dating back more than thirty years. Fortunately, the growth in computer power and recent algorithmic developments in chemical and computational physics enable us to proceed with validating, or improving, our MD simulations.

The measurement of interest to us is the osmotic coefficient of a solution composed of sodium chloride dissolved in water. The osmotic coefficient describes how strongly the sodium and chloride ions interact in the solvent. In the solution, there are many, many times the number of water molecules as ions, so the vast proportion of time required for any MD calculation to estimate the osmotic coefficient is heavily dominated by the water molecules, which ultimately do not play a role in the osmotic coefficient. Other research groups have developed methods for “coarse-graining” these MD simulations—in essence, to find simpler, reduced models of sodium and chloride in water, by fitting the reduced model to the (expensive) MD simulations. These less expensive models can then be used to calculate the osmotic coefficient at much reduced computational expense.

Our work has focused on calibrating a method known as inverse Monte Carlo (IMC), establishing which parameters are needed to ensure that the reduced models get the same answer as would be obtained from a truly massive MD simulation. These parameters include how many ions need to be included and how good an agreement needs to be established between the reduced model and the full MD simulations.

This year we used Jazz to run reproducibility experiments (10 large MD simulations for some of our tests) that are only rarely conducted in MD research. Our results underscore how important it is that independent MD simulations be conducted repeatedly, with statistics of their results reported, and just how misleading it can be to extrapolate from a single simulation. The IMC method is being widely used in so-called multiscale computations of biological membranes—very large simulations that in full MD are barely feasible, even with petaflop-scale computer clusters. We expect our results will strengthen the work of scientists who use IMC in this area, enabling them to check that their reduced models are truly converged and to verify the reproducibility of their simulations.

Computational Nanophotonics

PI: Stephen Gray (Center for Nanoscale Materials)

How can one control and manipulate light in nanoscale materials and devices? That is, how can one couple electromagnetic energy into these systems, concentrate and localize it, transport it, transform it, etc.? Answering such questions is of relevance to the development of future electronics devices, imaging, chemical and biological sensors, and solar energy, for example.

In collaboration with researchers from Troyes, France, we carried out simulations of how light can interact with long gold nanorods covered by a photo-responsive polymer. Experimental results on such systems had displayed a remarkable time-evolution of energetic hot spots on these rods. The simulations showed how the positions of the hot spots can change depending on the dielectric environment, that is, the evolving topology of the photo-responsive polymer. These results are important for learning how to precisely control the movement of energy in nanoscale systems.

With University of Chicago researchers, we simulated how light interacts with pairs of gold bipyramidal nanoparticles. In particular, it is possible for a force to result from such interactions that can either lead to a repulsive or attractive interaction between the nanoparticles. Understanding this force is important for the optical manipulation of small particles. Our numerically rigorous calculations showed how surface plasmon excitations (see Figure 19), corresponding to collective excitations of conduction electrons near the surfaces of the particles, can lead to particularly strong optical forces with wavelength tunability.

The calculations we have carried out have been in close collaboration with experimental groups and have assisted in both the interpretation and design of these state-of-the-art nanoscience experiments. Ultimately the combination of theory and experiment will yield not only new fundamental insights into how light interacts with metallic nanostructures, but show us how to manipulate energy at the nanoscale, which is relevant to a variety of applications areas (e.g., chemical sensing and solar energy).

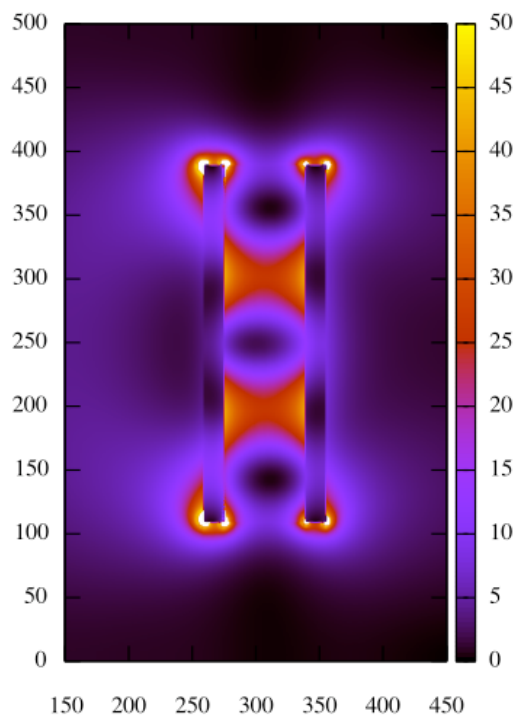


Figure 19: Image map of the strong electromagnetic field enhancements around a metal-insulator-metal nanostructure due to surface plasmon excitation. (Axis units are nanometers.) In the nanophotonics simulations on Jazz, such structures are studied in depth in order to learn how to manipulate electromagnetic energy at the nanoscale.

Publications and Presentations

M. L. Juan, Jrome Plain, Renaud Bachelot, Alexandre Vial, Pascal Royer, Stephen K. Gray, Jason M. Montgomery, and Gary P. Wiederrecht, Plasmonic electromagnetic hot spots temporally addressed by photoinduced molecular displacement, *J. Phys. Chem. A*, **113** (2009) 4647–4651.

R. Nome, M. J. Guffey, N. F. Scherer, and S. K. Gray, Plasmonic interactions and forces between Au bipyramid nanoparticle dimers, *J. Phys. Chem. A*, **113** (2009) 4408–4415.

Neocortical Seizure Simulation

PIs: Rick Stevens (Computing, Environment, and Life Sciences directorate) and Mark Hereld (Mathematics and Computer Science)

Epilepsy, a neurological disease characterized by repeated seizures, is the third most commonly diagnosed neurological disease. Its causes are likely many, and its genesis and development are not well understood. Ideally, one would like to record from many cells simultaneously in vivo to create a picture of how seizures start and spread from the focus. Unfortunately, current in vitro experimental recording techniques are time-consuming and are generally limited to a handful of

simultaneous recording sites or cells; they thereby provide an incomplete picture of the process at best. In vivo experiments are even more challenging.

We are attempting to overcome some of these limitations by investigating seizure generation in a scalable computational model of neocortex. This research complements clinical and laboratory work at the University of Chicago Hospitals. The cells and connectivity included in our model, though simplifications of reality, preserve what we consider the essential elements—multiple inhibitory and excitatory cell types, Hodgkin-Huxley-based ion channels, and several types of interneuron connections that vary in their topology and signaling speed. The model is built to help address a number of open questions in the field: Are seizures more of a cellular (ion channels) or network (connectivity) phenomenon? How small can a focus be? What conditions govern whether seizure-like behavior propagates or dies out?

During the past year, we compared the behavioral range of models based on realistic multicompartment neurons to that of networks based on simple integrate-and-fire (IAF) neurons. Using a model based on multicompartment neurons as reference, we studied how well (and in what sense) the IAF-based network can be made to duplicate the reference model. The work involved adapting existing techniques to this problem, systematically exploring the space of available parameters and issues, and developing methods for comparing the model responses analytically and visually.

We also applied a variant of a parameter estimation strategy recently proposed by H. Abarbanel to estimate cellular and network parameters in computational models of single neurons and neuronal networks. These models hold promise for smoothing the cost function surface associated with the space and therefore local minima. The project is ongoing, with modifications suggested by the earlier runs now being incorporated.

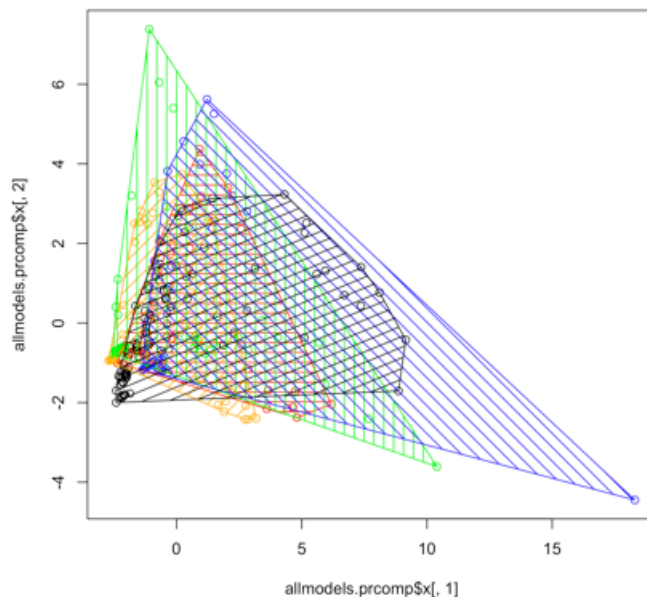


Figure 20. Data from four models and mouse data are compared in this 2D network behavior space. Each circle in the above diagram comes from a time series generated by a simulation or taken from lab data. Circles using the same model are the same color, differentiated only by model parameters.

Figure 20 shows data from four models and actual mouse data. For each time series a set of derived features are computed. The vector of these values is a new and compact representation of the time series. The set of all measured vectors is then subjected to PCA, from which the first two principal components are used to project the simulation data onto the 2D surface above, which we call a behavior space. We use the convex hull as an estimator of the subset of behaviors that can be reproduced by a given model. The intersection of two or more of these regions is an estimator of the set of behaviors that can be adequately represented by any of the models in that set. We hope that by understanding how to make such inferences reliably, we will be able to choose models that will answer our questions about a system with the lowest computational cost.

Publications and Presentations

Anne S. Warlaumont, Hyong C. Lee, Wim van Drongelen, Marc Benayoun, Rick L. Stevens, and Mark Hereld, Systematic comparison of the behaviors produced by models of epileptic neocortex, Poster presentation at *Third Epilepsy Symposium: Tools of Epilepsy Research*, Chicago, 2009.

W. Van Drongelen, J. Dwyer, H.C. Lee, A. Martell, R. Stevens, and M. Hereld, Oscillations in a network model of neocortex, in *Proceedings of the European Symposium on Artificial Neural Networks*, 2009, pp. 425-430.

Optimization of Many-Body Wavefunctions

PI: Richard Chasman (Physics)

The purpose of our work in optimization of many-body wavefunctions is to obtain a good description of low-lying nuclear states, going beyond a mean-field approximation when the nucleus of interest is transitional (e.g., transitional between a spherical shape and a deformed shape). The immediate problem being addressed is the behavior of nuclei in the region of the periodic table characterized by roughly equal numbers of protons and neutrons. These nuclei have many very anomalous features, such as the Wigner energy and large interlevel spacings. An important aspect of this work is developing new techniques to deal with the nuclear many-body problem and the general quantum mechanical many-body problem. We are developing a variational configuration-interaction method to treat these problems.

In 2009, we extended our variational configuration-interaction method to handle excited states having the same quantum numbers as the ground state. The results, for excited states and ground states, are in excellent agreement with experiment. See Figure 21.

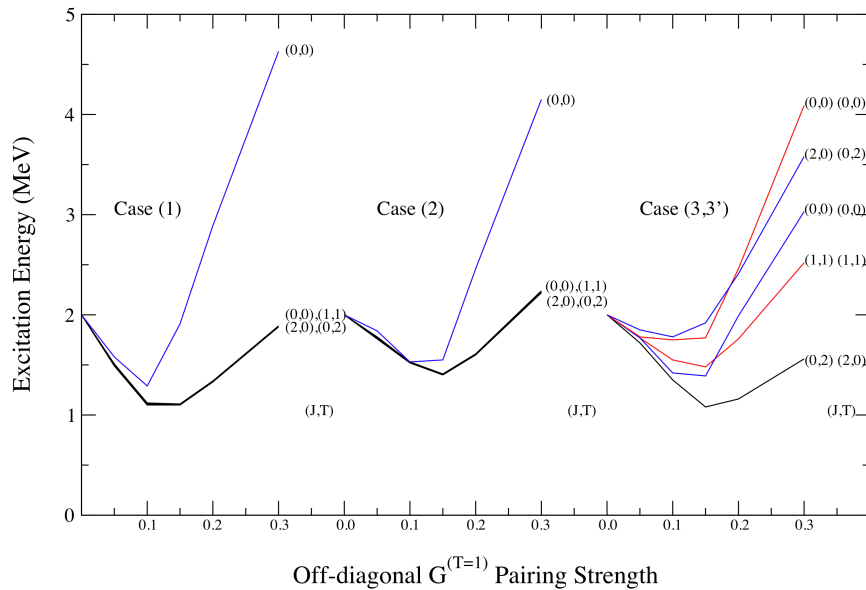


Figure 21: Effects of different assumptions about the details of the interaction on the excited state spectrum. Case 1 is the excited state spectrum calculated when all pairing matrix elements are taken to be equal. In Case 2, diagonal pairing matrix elements are taken to be 2.4 times the off diagonal pairing matrix elements. There are good physical grounds for this assumption. In Case 3, $T=0$ pairing neutron-proton matrix elements are taken to be 10% smaller than the other pairing matrix elements and in Case 3', the $T=1$ matrix elements are reduced by 10%. Additionally, in Cases 3 and 3', diagonal elements are 2.4 times the off-diagonal elements. The results show the sensitivity of the calculated excitation spectrum to the details of the interaction.

Publications and Presentations

R. Chasman and P. van Isacker, Pair-vibrational states in the presence of neutron-proton pairing, preprint, 2009.

Parallel Tools Performance Testing

PIs: Robert Latham and Robert Ross (Mathematics and Computer Science)

The Parallel Tools project continues to develop and study highly scalable software tools and libraries for parallel applications. Our efforts include a parallel file system (PVFS), an MPI-2 implementation (MPICH2), an MPI-IO implementation (ROMIO), and work on higher-level libraries (Parallel-NetCDF). These projects as a whole both provide a way to expose the performance of underlying hardware and enable application writers to write “performance portable” code that can work well on the wide variety of high-performance computing resources available today, as well as the new designs of the future.

In 2009, we used Jazz as a “sanity check” environment to ensure that PVFS, MPICH2, Parallel-NetCDF, and experimental software packages ran on a wide variety of systems. Specifically, we

built and tested PVFS nightly in the Jazz environment, catching regressions in our GM support. We also used Jazz to test both PVFS at scale. PVFS scalability testing benefits all Jazz users because it is the high-performance file system used in the cluster.

Parallel Implicit Algorithms in Edge Fusion Simulations

PI: Lois Curfman McInnes (Mathematics and Computer Science)

We are developing scalable algorithms for the solution of nonlinear partial differential equations that arise in the multi-institutional SciDAC FACETS (Framework Application for Core-Edge Transport Simulations) project. This project's aim is the construction of a multiphysics, parallel framework application that will enable whole-device modeling for the U.S. fusion program and ITER, the next-step fusion confinement device.

Our FACETS work on scalable nonlinear solvers focuses on exploring issues in implicit Newton-based solution strategies in the edge plasma transport applications UEDGE and BOUT and the Scalable Nonlinear Equation Solvers package in PETSc. We have used Jazz for experiments to compare the efficiency and scalability of various preconditioning algorithms for UEDGE. The use of PETSc enabled scientists to overcome a major bottleneck in the parallel implementation of UEDGE, opening an array of possible preconditioners that allow scientists to advance both ions and neutrals together.

Work during 2009 focused on extending parallel interfaces for the edge plasma application UEDGE and the nonlinear solvers in the PETSc. Also, because the FACETS project is transitioning from use of the original BOUT edge turbulence application to a new variant, BOUT++, during 2009 we developed a new interface between PETSc and BOUT++.

Publications and Presentations

J. R. Cary, J. Candy, J. Cobb, R. H. Cohen, T. Epperly, D. J. Estep, S. Krasheninnikov, A. D. Malony, D. C. McCune, L. C. McInnes, A. Pankin, S. Balay, J. A. Carlsson, M. R. Fahey, R. J. Groebner, A. H. Hakim, S. E. Kruger, M. Miah, A. Pletzer, S. Shasharina, S. Vadlamani, D. Wade-Stein, T. D. Rognlien, A. Morris, S. Shende, G. W. Hammett, K. Indireskumar, A. Pigarov, and H. Zhang, Concurrent, Parallel, Multiphysics coupling in the FACETS project, *J. Phys.: Conf. Ser.*, **180** (2009) 012056.

L. C. McInnes, Parallel implicit solvers in large-scale computational science, Invited 45-minute topical presentation, *2009 SIAM Annual Meeting*, Denver, July 9, 2009.

L. McInnes, S. Farley, T. Rognlien, M. Umansky, and H. Zhang (speaker), Progress in parallel implicit methods for tokamak edge plasma modeling, Invited presentation in minisymposium at the *2009 SIAM Conference on Computational Science and Engineering*, Miami, Florida, March 2–6, 2009.

Quantum Monte Carlo Calculations of Light Nuclei

PIs: Ivan Brida, Stefano Gandolfi, Kenneth M. Nollett, Steven C. Pieper, Muslema Pervin, and Robert B. Wiringa (Physics)

This project uses quantum Monte Carlo—Green’s function (GFMC), variational (VMC), and auxiliary-field diffusion (AFDMC)—methods to compute ground-state and low-lying excited-state expectation values of energies, densities, structure functions, astrophysical reaction rates, and so forth, for light nuclei and low-energy scattering reactions involving these nuclei. Realistic two- and three-nucleon potentials are used. Our goal is a description of all of these systems using a Hamiltonian that also provides an excellent description of nucleon-nucleon scattering and nucleonic matter. Such a “standard nuclear model” can then be used, for example, to compute low-energy astrophysical reactions that cannot be experimentally measured.

During 2009 Jazz was used for many aspects of this project (see Figure 22). The fast turnaround of Jazz makes it the machine of choice for all but our biggest calculations, which are done on the Blue Gene/P. The specific projects this year fell into four categories.

1. Transition matrix elements

One of our goals is to reliably compute the matrix elements that determine the rates of nuclear decays in light nuclei. These include the magnetic dipole and electric quadrupole matrix elements for photon emission and the Fermi and Gamow-Teller matrix elements for weak decay. During the latter part of FY08 and early FY09 we added two-body meson-exchange current corrections to our study of 15 transitions in $A=6,7$ nuclei, which are fixed in magnetic moment calculations; the M1 transitions are now in excellent agreement with experiment. Additional calculations of various transitions in $A=8-10$ nuclei were made during 2009, and we successfully proposed a joint project with experimentalists working at the Argonne Tandem Linac Accelerator System (ATLAS) to study transitions in $A=10$ nuclei.

2. Spectrum of $A=9,10$ nuclei and cluster-cluster overlaps

We continued expanding our VMC and GFMC calculations of excitation spectra in light nuclei in 2009. The largest nuclei that are feasible to study on Jazz are $A=9,10$ nuclei; larger systems like ^{12}C require the Blue Gene/P. We have previously calculated ground states and low-lying excited states in $A=9,10$. Our new work focused on the unnatural-parity single-intruder states, like the positive-parity states in ^9Be , and both single- and double-intruder states in ^{10}Be and ^{10}B . New variational trial functions are being developed that emphasize the underlying cluster structure; for example, ^9Be is very much an alpha-alpha-n system. This work also supports the new experimental work on transitions described above.

We also continued work on cluster-cluster overlaps. In the past several years we have made many calculations of overlaps that measure the probability that an A -body nucleus with total spin J looks like an $(A-1)$ -body nucleus with spin J' and a single nucleon with total angular momentum j . These overlaps serve as input to distorted-wave Born approximation reaction calculations that help interpret a number of experiments at ATLAS and other facilities. During 2009, we started extending the calculations to two-nucleon overlaps. We expect these to improve our understanding of the cluster structure of nuclei such as ^6He and ^{10}Be and expand the range of experiments we can help interpret.

3. Dependence of nuclear binding on hadronic mass variation

Some grand unified theories predict that fundamental “constants” such as the electromagnetic fine structure constant or bare quark masses could vary temporally or spatially during the course of

the universe's evolution. There are hints of such variation in quasar absorption spectra, the Oklo natural nuclear reactor, and big bang nucleosynthesis. In 2007 we made a first study of how nuclear binding energies would vary if the input hadron (nucleon, nucleon resonance, pion, and vector meson) masses varied with changes in the underlying bare quark mass. In 2008-2009 we extended our studies to low-lying excited states, to explore how spin-orbit splittings of nuclear levels in $A=5-9$ nuclei would be affected by quark mass variations. We obtained rough estimates for much larger nuclei like ^{150}Sm and ^{229}Th , which could provide very sensitive tests of time variation of some fundamental constants.

4. Neutron drops

Neutron drops are collections of neutrons interacting via a standard NN and 3N Hamiltonian with an added artificial external well. The well can be adjusted to change the density or surface thickness, and it can be nonspherical. If the NN and 3N part of the Hamiltonian is realistic, the energies and density profiles from such calculations can provide useful input to energy-density functionals (EDF). Our GFMC method is limited to only 14 neutrons in the well because of its exponential growth with the number of neutrons. The AFDMC method has only a power-law growth and can do up to 100 neutrons, but it may be less accurate. We have used Jazz to compute up to 20-neutron drops by AFDMC for comparison with the GFMC calculations for similar systems. They are also being compared to Skyrme EDFs as part of the SciDAC UNEDF (Universal Nuclear EDF) project.

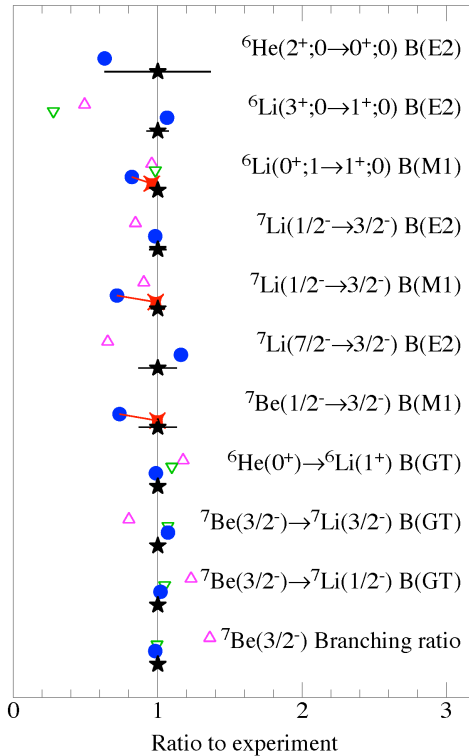


Figure 22. Ratio of calculated to measured transition rates for $A=6,7$ nuclei. Magenta open (up) triangles are from the traditional Cohen-Kurath $1p$ shell model, green open (down) triangles are no-core shell model (NCSM), solid blue circles are GFMC calculations in impulse approximation, the red fort symbols are GFMC with MEC corrections added (M1 transitions only), and black stars with error bars are experimental values.

Publications and Presentations

V. V. Flambaum and R. B. Wiringa, Enhanced effect of quark mass variation in ^{229}Th and limits from Oklo data, *Phys. Rev. C*, **79** (2009) 034302-1:8.

E. A. McCutchan, C. J. Lister, R. B. Wiringa, S. C. Pieper, D. Seweryniak, J. Greene, C. J. Chiara, M. P. Carpenter, R. V. F. Janssens, T. L. Khoo, T. Lauritsen, I. Stefanescu, and S. Zhu, Precise electromagnetic tests of ab initio calculations of light nuclei: States in ^{10}Be , *Phys. Rev. Lett.*, **103** (2009) 192501.

K. M. Nollett, Quantum Monte Carlo methods, Presentation at the *Workshop on Continuum Coupling Close to the Drip Lines*, CEA Saclay, Gif-sur-Yvette, France, May 18-20, 2009.

R. B. Wiringa, Nuclear quantum Monte Carlo, effective field theories and the many-body problem, Presentation at the *Institute for Nuclear Theory Program INT-09-1*, University of Washington, Seattle, Washington, March 23–June 5, 2009.

R. B. Wiringa, Recent developments in nuclear quantum Monte Carlo, Presentation at the *Bulk Nuclear Properties 5th ANL/MSU/JINA/INT FRIB Workshop*, East Lansing, Michigan, November 19-22, 2008, AIP Conf. Proc. 1128, 1-10 (2009)

Safety Analysis Report Review of Radioactive Material Packaging

PI: Kun Chen (Decision and Information Sciences)

The Packaging Certification and Life-Cycle Management Group (PCLCM) at Argonne helps ensure the safety of packaging for radioactive and fissile materials. In 2009, we used Jazz to analyze two nuclear material packagings: the Model 9516 and Model 9979. The former is used to transport plutonium dioxide heat source material both domestically and internationally; the latter is used to transport uranium metals, oxides and other solid compounds. In particular, we ran the MCNP and SCALE codes to evaluate radiation shielding and nuclear criticality safety. Because Jazz has multiple nodes, we were able to run different models at the same time. This capability enabled us to simulate different situations and configurations during the transport in a timely manner. Our work helped DOE complete the radiation shielding evaluation of the 9516 packaging enabled Idaho National Laboratory to receive plutonium heat source materials from Russia, while protecting worker safety and public health (see Figure 23).

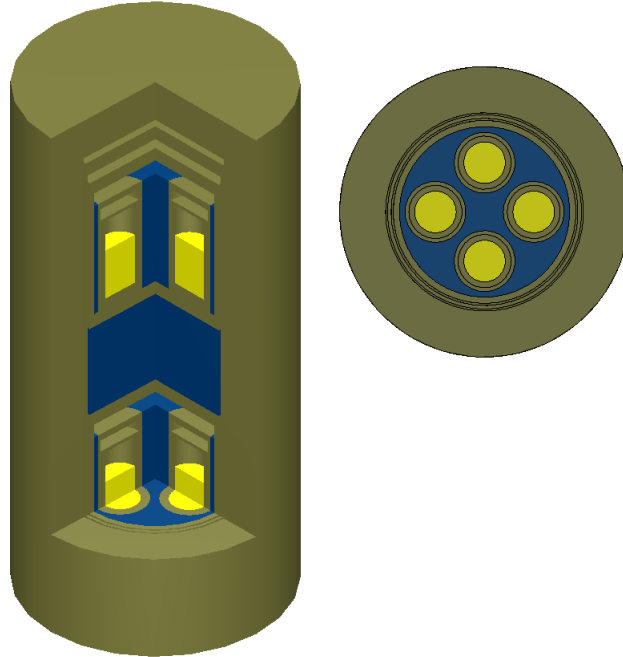


Figure 23: Radiation shielding model of 9516 packaging.

Toolkit for Advanced Optimization

PIs: Todd Munson and Jason Sarich (Mathematics and Computer Science)

The goal of the Toolkit for Advanced Optimization (TAO) project is to provide a portable numerical optimization library for large-scale scientific applications. To achieve this goal, we install, debug, test, and run applications on a variety of parallel architectures, including Jazz. During the past year, using 73 processors on Jazz, we compared the current TAO algorithm for derivate-free optimization to a newly developed algorithm (Pounder) and determined that the addition of this algorithm to TAO would create a significant improvement.

Publications and Presentations

J. Sarich, TAO tutorial, Presentation at the *Tenth Workshop on the DOE ACTS Collection*, Lawrence Berkeley National Laboratory, August 18–21, 2009.

Uncertainty in Weather Forecasting

PI: Emil Constantinescu (Mathematics and Computer Science)

This project focuses on wind-speed forecast and uncertainty quantification using the Weather Research and Forecast (WRF) model. The uncertainty of the wind-speed forecast is modeled by using a sampling technique that generates an ensemble of the future realizations in the targeted geographical region (in our case, Illinois; see Figure 24). The ensembles are obtained by using a scalable implementation on a distributed-memory parallel computing, and the wind-power realizations are exploited through a stochastic unit commitment/energy formulation. The most expensive computational element is the evolution of each individual member.

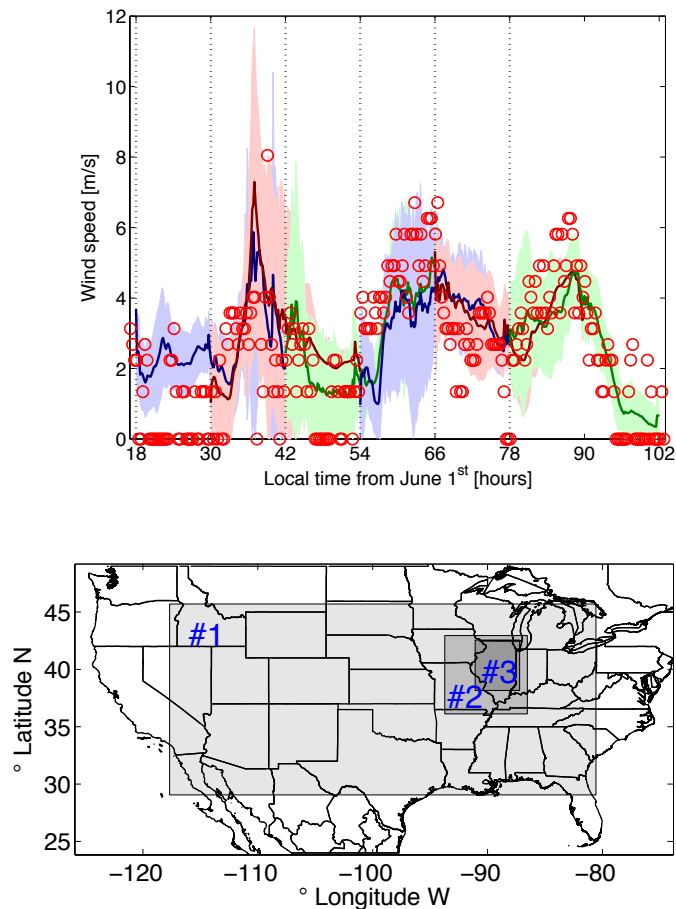


Figure 24: Wind speed ($\pm 2\sigma$) predictions and measurements for Chicago (June 2006). Each ensemble evolves for 24 hours, and new ones are started every 12 hours. These results indicate very good predictive and uncertainty capabilities.

We therefore consider a two-level parallel implementation scheme in which each member runs in parallel and is independent from the others. This approach yields a highly scalable solution (see Figure 25). We validate the forecast information using real wind-speed data obtained from a set of meteorological stations in Illinois and use this forecast information to perform an economic analysis of the impact of increasing adoption levels of wind power on a simulated power generation system.

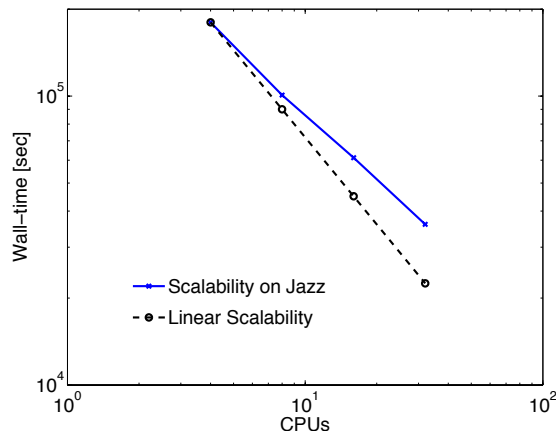


Figure 25: *Scalability on Jazz.*

Our computational study has identified several issues and limitations that are not present in idealized experiments using artificial uncertainty information. Moreover, our inference strategy shows that 30 WRF realizations are sufficient to produce a good estimate of the optimal cost. These computations indicate, through a proof of concept, that uncertainty estimation and forecast of ambient conditions using numerical weather prediction models are both computationally feasible and critical in achieving high adoption levels of renewable (wind) energy resources.

Publications and Presentations

Emil M. Constantinescu, Victor M. Zavala, Matthew Rocklin, Sangmin Lee, and Mihai Anitescu, A computational framework for uncertainty quantification and stochastic optimization in unit commitment with wind power generation, Preprint ANL/MCS-P1681-1009, 2009.

Optimization of Nuclear-Energy DFT Functionals

PI: Jorge Moré (Mathematics and Computer Science)

One of the goals of the UNEDF (Universal Nuclear Energy Density Functional) SciDAC project is the improvement of current density functional theory (DFT) functionals so that theoreticians can better predict the properties and behavior of atomic nuclei over the entire nuclear table. The aim is to replace current phenomenological models of nuclear structure and reactions with a well-founded microscopic theory that delivers maximum predictive power with well-quantified uncertainties. The long-term vision is to arrive at a comprehensive and unified description of nuclei and their reactions, grounded in the fundamental interactions between the constituent nucleons.

Evaluating a DFT functional for a set of parameters requires running an expensive simulation, one for each nucleus. We are currently performing optimizations using less than 10% of the nuclei (approximately 100 nuclei). Hence, evaluation of a functional of 100 nuclei at a particular parameter set requires up to 30 CPU-hours, and the optimization over 12 parameters can require

200–300 such evaluations, giving a total of 6,000-9,000 CPU-hours for each version of the functional we want to optimize. Thus, it is important to find acceptable parameter values with the least number of function evaluations.

To this end, we have been developing a new model-based optimization algorithm (Pounder) that determines trial parameters by minimizing a model (or surrogate) of the functional. Pounder modifies the trial parameters and the model of the functional until convergence is achieved or the computational budget is exhausted. Our results show (see Figure 26) that Pounder is able to find suitable parameter values whereas the best current algorithm (Nelder-Mead) fails. For example, in one of our benchmarking runs we found that the Nelder-Mead method did not find an acceptable solution after 4300 CPU-hours. On the other hand, Pounder found an acceptable solution after 216 CPU-hours. This development makes possible the calibration of expensive simulations.

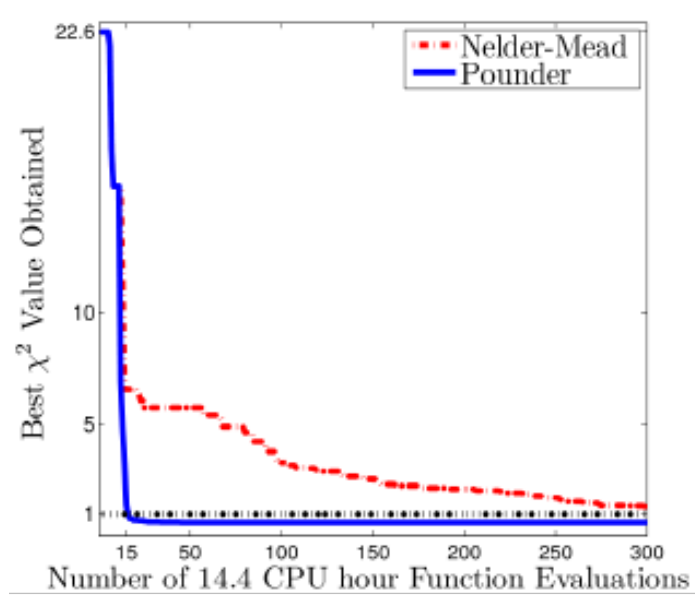


Figure 26: Performance of the classic Nelder-Mead method and our Pounder solver on an HFBTHO parameter estimation problem. Since each chi-squared function evaluation requires 14.4 CPU-hours, Pounder obtains an acceptable solution within 9 CPU-days (15 evaluations) while Nelder-Mead is unable to obtain an acceptable solution within 180 CPU-days (300 evaluations).

We have obtained the first optimization and sensitivity analysis for a new class of DFT functionals developed by our collaborators at Oak Ridge. Some of these processes are inherently sequential and hence admit limited scaling. While we utilize leadership-class computing systems, Jazz provides essential resource for our tests using between 16 and 100 processors. The availability of MATLAB on Jazz also allows us to test prototype algorithms on challenging breakthrough problems. Our work has generated considerable excitement in the UNEDF project, and as a result the request for optimization capabilities is growing.

Publications and Presentations

J. Dobaczewski, W. Satula, B. Carlsson, J. Engel, P. Olbratowski, P. Powalowski, M. Sadziak, J. Sarich, N. Schunck, A. Staszczak, and others, Solution of the Skyrme-Hartree-Fock-Bogolyubov

equations in the Cartesian deformed harmonic-oscillator basis, HFODD (v2. 38j): A new version of the program, Arxiv preprint arXiv:0903.1020, 2009.

J. Moré, Optimization strategies for complex UNEDF simulations, Presentation at the *UNEDF Workshop*, Pack Forest, Washington, June 22-25, 2009.

J. Moré, “Recent developments in parameter estimation for complex simulations,” Third LACM-EFES-JUSTIPEN Workshop, Joint Institute for Heavy Ion Research, Oak Ridge National Laboratory, February 23–25, 2009.

M. Stoitsov, J. Moré, W. Nazarewicz, J. C. Pei, J. Sarich, N. Schunck, A. Staszczak, and S. Wild, Towards the universal nuclear energy density functional, *Journal of Physics, Conference Series*, **180** (2009) 012082.

S. Wild, Derivative-free optimization for DFT: A view from the trenches of HFBTHO calibration, Presentation at the *UNEDF Workshop*, Pack Forest, Washington, June 22–25, 2009.

S. Wild, Model-based optimization algorithms for expensive simulation-driven problems, Presentation at *Iowa State University Nuclear Physics Seminar*, Ames, Iowa, March 5, 2009.

S. Wild, Skyrme functional fitting at 13% of the computational expense, Presentation at the *Third LACM-EFES-JUSTIPEN Workshop*, Joint Institute for Heavy Ion Research, Oak Ridge National Laboratory, February 23–25, 2009.

S. Wild, Turning weeks into days: Parameter estimation for expensive nuclear energy density functionals, Presentation at the *Argonne Postdoctoral Research Symposium*, Argonne National Laboratory, September 10, 2009.

Multimethod Linear Solvers in Large-Scale PDE-Based Simulations

PIs: B. Norris, L. McInnes (Mathematics and Computer Science)

Many large-scale scientific simulations involve the parallel solution of time-dependent and/or nonlinear partial differential equations. Overall simulation time is often dominated by the parallel solution of large-scale, sparse linear systems. Typically, application developers select a particular algorithm to solve a given linear system and keep this algorithm fixed throughout the simulation. However, it is difficult to select a priori the most effective algorithm for a given application. Moreover, for long-running applications in which the numerical properties of the linear systems change as the simulation progresses, a single algorithm may not be best throughout the entire simulation. We are therefore exploring *polyalgorithmic multimethod linear solvers* in the context of several parallel applications, including flow in a driven cavity, compressible Euler flow, radiation transport, and edge plasma simulations to potentially improve the execution time and reliability of linear system solution. We are investigating an adaptive, polyalgorithmic approach, where the solution method is selected dynamically to match the attributes of the linear systems as they change during the course of a simulation.

During 2009 we focused on developing component database capabilities that link measurement and analysis infrastructure and control infrastructure for dynamic component replacement and domain-specific decision making. We are just beginning to explore ideas in multimethod solvers research within new multi-institutional SciDAC collaborations in fusion and accelerator modeling via the projects FACETS (Framework Application for Core-Edge Transport Simulations) and COMPASS (Community Petascale Project for Accelerator Science and Simulation). We are developing capabilities for monitoring, checkpointing, and gathering of performance data, which may be managed through two types of databases. The first is created and destroyed during runtime and stores performance data for code segments of interest, as well as various application-specific performance events in the currently running application instance. The second database is persistent and contains performance data from various applications and different instances of the same application. This database can also contain performance information derived through offline analysis of raw data.

Figure 27 is an illustration of this work as applied to applications in quantum chemistry. Our efforts to date have been setting the stage for future applications in this area.

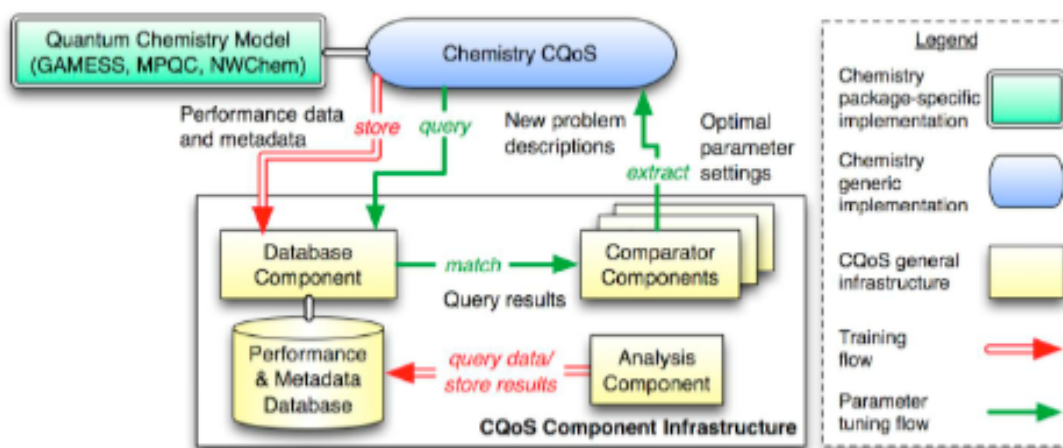


Figure 27: Components and parameter tuning flow in a computational quality-of-service (CQoS)-enabled quantum chemistry application.

Publications and Presentations

L. Li, J. Kenny, M-S. Wu, K. Huck, A. Gaenko, M. Gordon, C. Janssen, L. C. McInnes, H. Mori, H. Netzloff, B. Norris, and T. Windus, Adaptive application composition in quantum chemistry, in *Proceedings of the 5th International Conference on the Quality of Software Architectures*, East Stroudsburg University, Pennsylvania, June 22–26, 2009.

S. Muszala, J. Amundson, L. C. McInnes, and B. Norris, Two-tiered component design and performance analysis of Synergia2 accelerator simulations, accepted for publication in the *Proceedings of CBHPC09*, August 2009.



Argonne National Laboratory

9700 South Cass Avenue
Argonne, IL 60439

www.anl.gov

www.lcrc.anl.gov



U.S. DEPARTMENT OF
ENERGY

Argonne National Laboratory is a
U.S. Department of Energy laboratory
managed by UChicago Argonne, LLC